INSTITUTO POTOSINO DE INVESTIGACIÓN CIENTÍFICA Y TECNOLÓGICA, A.C.

POSGRADO EN CIENCIAS EN BIOLOGIA MOLECULAR

Phenotypic characterization of contemporaneous clinical isolates of *Candida glabrata*

Tesis que presenta

Erandi Litzey Robles López

Para obtener el grado de

Maestra en Ciencias en Biología Molecular

Codirectores de la Tesis:
Dra. Irene Beatriz Castaño Navarro
Dr. Marco Josué Hernández Chávez

San Luis Potosí, S.L.P., Junio de 2026

Constancia de aprobación de la tesis

La tesis "**Phenotypic characterization of contemporaneous clinical isolates of *Candida glabrata***" presentada para obtener el Grado de Maestra en Ciencias en Biología Molecular fue elaborada por **Erandi Litzey Robles López** y aprobada el **09 de junio de 2026** por los suscritos, designados por el Colegio de Profesores de la División de Biología Molecular del Instituto Potosino de Investigación Científica y Tecnológica, A.C.

_____

Dra. Irene Beatriz Castaño Navarro
Codirectora de la tesis

_____

Dr. Marco José Hernández Chávez
Codirector de la tesis

_____

Dra. Fabiola Jaimes Miranda
Miembro del Comité Tutoral

_____

Dr. Francisco Elihu Bautista Redonda
Miembro del Comité Tutoral

Créditos Institucionales

Instituto Potosino de Investigación Científica y Tecnológica, A. C.
Esta tesis fue elaborada en el Laboratorio de Microbiología Molecular de la División de Biología Molecular del Instituto Potosino de Investigación Científica y Tecnológica, A.C., bajo la codirección de la Dra. Irene Beatriz Castaño Navarro y el Dr. Marco Josué Hernández Chávez.

Durante la realización del trabajo el autor recibió una beca académica del Consejo Nacional de Ciencia y Tecnología 2059982 y del Instituto Potosino de Investigación Científica y Tecnológica, A. C.

Este trabajo fue apoyado por el proyecto No. 2024-03-M28 del Fondo: Multas Electorales Convocatoria 2024-03. Proyectos de Investigación, Desarrollo e Innovación, otorgado a Irene Beatriz Castaño Navarro.

Esta tesis contó con el apoyo del Laboratorio Nacional de Biotecnología Agrícola, Médica y Ambiental (LANBAMA), el Laboratorio de Genómica Funcional y Comparativa y el Laboratorio de Biología Molecular de Plantas.

Dedicatorias

A mi **Tita**, por todo el amor que me ha dado y me ha hecho crecer en esta y en todas mis etapas.

A mi papá, **Sergio**, por contagiarme del ánimo necesario para impulsarme a logar los proyectos que me planteo.

A mis tías y tíos, **Katty**, **Anllely**, **César** y **Martín**, por fungir para mí como figuras de inspiración para la superación de muchas de mis metas.

A mis hermanos, **Frigman**, **Yesli**, **Sergio** y **Roberto**, y a mis primos que también se sienten como mis hermanos, **Mairany**, **Skarlet**, **Anyelo** y **Jatziry**, por acompañarme de diferentes maneras en todos los cambios que conllevó todo este trabajo.

A **Jorge**, por creer en mí y llenarme de determinación para muchas de las decisiones que me llevaron a esto.

A la **Polen** y el **Güero**, por ser el apoyo incondicional que nunca me faltó, manifestado en cuatro patitas.

A mis amigos, especialmente a **Zuli**, **Roger**, **Lili**, **Aby** y **Ramón,** porque que han confiado en mí siempre, incluso más que yo misma.

A **Yessi**, **Hugo** y a sus maravillosos hijos, **Maxi**, **Isabela** y **Amaia**, porque me dejaron encontrar en ellos un apoyo muy reconfortante y familiar durante estos últimos años, ensañándome así un camino y muchas metas que ahora quiero alcanzar.

A todos mis compañeros de la **23ª generación de maestría en biología molecular**, por todas las experiencias, el acompañamiento y el respaldo que me mostraron durante este tiempo, realmente sin ustedes esto no hubiera sido lo mismo.

Agradecimientos

A la **SECIHTI**, por el apoyo económico brindado a través de la beca que hizo posible la realización de mis estudios de posgrado.

Al **Instituto Potosino de Investigación Científica y Tecnológica A.C.**, por el respaldo institucional y las facilidades otorgadas para el desarrollo de este trabajo.

Al **Laboratorio Nacional de Biotecnología Agrícola, Médica y Ambiental** (LANBAMA)**,** al **Laboratorio de Genómica Funcional** y **Comparativa y al Laboratorio de Biología Molecular de Plantas**, por el apoyo técnico y los servicios proporcionados durante la ejecución de este proyecto.

A la **Dra. Irene Castaño Navarro**, por compartir generosamente sus conocimientos y experiencia. Gracias por ser un ejemplo tanto en el ámbito científico como humano, por creer en mis capacidades y por despertar y fortalecer en mí la pasión por la investigación científica.

Al **Dr. Marco Josué Hernández Chávez**, por su orientación constante a lo largo de este trabajo, por su paciencia, dedicación y valiosas contribuciones, y especialmente por su disposición permanente para apoyarme y acompañarme en los momentos de mayor dificultad.

A la **Dra. Fabiola Jaimes Miranda** y al **Dr. Francisco Elihú Bautista Redonda**, por sus observaciones y recomendaciones, las cuales enriquecieron este trabajo y contribuyeron de manera importante a mi formación profesional.

Al **Dr. Alejandro De Las Peñas**, por sus valiosos conocimientos, sugerencias e ideas, que representaron una aportación significativa para el desarrollo de este proyecto.

A la **Dra. Ma. Guadalupe Gutiérrez Escobedo**, por su dedicación al enseñarme las técnicas de laboratorio y por los consejos que contribuyeron a mi crecimiento académico y profesional.

Al **Dr. Nicolas Gómez Hernández**, por su acompañamiento, apoyo y asesoría técnica durante el desarrollo de esta investigación.

A **Gloria López Niño**, por su invaluable apoyo para la realización de los experimentos que hicieron posible la obtención de los resultados de este trabajo.

A mis compañeros del Laboratorio de Microbiología Molecular, especialmente a **Ana, Lili, Yaz, Laura, Alex y Oscar**, por compartir conmigo sus conocimientos, experiencias y amistad, haciendo de esta etapa una experiencia enriquecedora.

A mis compañeros de **la 23.ª generación de la Maestría en Biología Molecular**, por las experiencias compartidas, el apoyo constante y la compañía brindada a lo largo de este camino; su presencia hizo que esta etapa fuera mucho más significativa y enriquecedora.

Contenido

Lista de tablas

Lista de figuras

Anexos

Abreviaturas

AN-	Isolate from the Instituto Nacional de Ciencias Médicas y Nutrición Salvador Zubirán followed by the corresponding number
bp	Base pair
CSP	Caspofunginb
CSP^R	Caspofungin resistant
FLC	Fluconazole
FLC^{SDD}	Fluconazole susceptible dose-dependent
FLC^R	Fluconazole resistant
FPPL	Fungal Pathogens Priority List
GLY-	Unable to use the non-fermentable carbon source, glycerol
GLY+	Able to use the non-fermentable carbon source glycerol
H2O2	Hydroxen peroxide
IAH	Independent Action Hypotesis
MIC	Minimum Inhibitory Concentration
MIC_{50}	Minimum Inhibitory Concentration at which 50% of a specific population is inhibited from growth under different antifungals
MICA	Micafungin
MLP	Microsatellite Length Polymorphism
OD_{600}	Optical Density at wavelength of 600 nm
P-	Patient followed by the corresponding number
SDS	Sodium dodecyl sulfate
TTC	Triphenyltetrazolium Chloride
WHO	World Health Organization
YPD	Yeast extract Peptone Dextrose
YPE	Yeast extract Peptone Ethanol
YPG	Yeast extract Peptone Glycerol

Resumen
Caracterización fenotípica de aislados clínicos contemporáneos de *Candida glabrata*

Candida glabrata es un importante patógeno oportunista debido a su capacidad para adaptarse rápidamente a los ambientes del hospedero y desarrollar resistencia antifúngica. Estudios recientes han demostrado que cepas aisladas de una misma muestra clínica en un mismo punto temporal que comparten un origen clonal, conocidas como cepas contemporáneas, pueden presentar variabilidad fenotípica y genotípica desde las etapas iniciales de la infección. En este contexto, analizamos aislados clínicos contemporáneos de *C. glabrata* obtenidos de diferentes pacientes (P6, P8 y P10) para determinar si existe variabilidad genotípica y fenotípica entre los aislados derivados del mismo episodio infeccioso. Se seleccionó un total de 40 aislados contemporáneos derivados de muestras sanguíneas de los tres pacientes. Se determinó si tienen un origen clonal mediante genotipificación por polimorfismos en la longitud de microsatélites (MLP), utilizando los marcadores moleculares *RPM2*, *MT-I* y *ERG3*, además de las regiones microsatélite de *EPA1*. La caracterización fenotípica bajo múltiples condiciones de estrés mostró perfiles de respuesta similares entre los aislados contemporáneos del P8. Los aislados contemporáneos del P10 mostraron crecimiento reducido en fuentes de carbono no fermentables, pero conservaron la función respiratoria mitocondrial. Los aislados del P6 mostraron diferencias de crecimiento bajo estrés por fluconazol, sin embargo, la determinación de la MIC_{50} mediante dos métodos no mostró diferencias significativas de susceptibilidad para fluconazol, caspofungina o micafungina. Los tiempos de duplicación en presencia de fluconazol sí muestran algunas diferencias entre dos aislados contemporáneos del P6, lo que sugiere la aparición temprana de variabilidad fenotípica entre estos. Esta variabilidad podría contribuir a la subestimación de las interacciones antifúngicas en el contexto clínico, lo que podría resultar en tratamientos ineficaces y la posterior adquisición de resistencia frente a antifúngicos de primera línea.

Palabras clave: Aislados contemporáneos, *Candida glabrata*, Resistencia antifúngica, Variabilidad fenotípica y genotípica

Abstract

Phenotypic characterization of contemporaneous clinical isolates from *Candida glabrata*

Candida glabrata is an important opportunistic pathogen due to its ability to rapidly adapt to host environments and develop antifungal resistance. Recent studies have shown that strains isolated from the same clinical sample at the same time point and sharing a clonal origin, known as contemporaneous strains, may exhibit phenotypic and genotypic variability from the early stages of infection. In this context, we analyzed contemporaneous clinical isolates of C*. glabrata* obtained from different patients (P6, P8, and P10) to determine whether genotypic and phenotypic variability exists among isolates derived from the same infectious episode. We selected 40 contemporaneous isolates derived from blood samples from the three patients and determined whether they share a clonal origin by microsatellite length polymorphism (MLP) genotyping using the molecular markers *RPM2*, *MT-I*, and *ERG3*, as well as the *EPA1* microsatellite regions. Phenotypic characterization under multiple stress conditions showed similar response profiles among contemporaneous isolates from P8. Contemporaneous isolates from P10 showed reduced growth on non-fermentable carbon sources but preserved mitochondrial respiratory function. Isolates from P6 showed differential growth under fluconazole stress; however, MIC_{50} showed no significant differences in susceptibility to fluconazole, caspofungin, or micafungin using two methods. Duplication times in the presence of fluconazole did show some differences between two contemporaneous isolates from P6, which suggests the early emergence of phenotypic variability among them. This variability could contribute to the underestimation of antifungal interactions in clinical settings and possibly leading to ineffective treatments and the subsequent acquisition of resistance to first-line antifungal agents.

Keywords: Contemporaneous isolates, Candida glabrata, Antifungal resistance, Phenotypic and genotypic variability

1. Introduction

Globally, fungal infections are responsible for approximately 1.7 billion cases of superficial infections, such as dermatitis. In addition invasive fungal infections (IFIs) cause nearly 1.5 million deaths annually [1]. Although fungal infections substantially contribute to human morbidity and mortality, the impact of these diseases on human health is not widely appreciated and deaths resulting from these infections are often overlooked [2]. Among the etiological agents, the genus *Candida* is particularly relevant and represents the second most frequent group of fungal pathogens worldwide [3].

Candida species (*Candida* spp.) are the most common fungal etiological agent of life-threatening invasive infections in patients who are severely immunocompromised, who have endured invasive clinical procedures, or who have experienced major trauma, and treatment requires extended stays in intensive care units [4–6]. Candidemia and other forms of invasive candidiasis are the most important of the invasive mycoses [7].

In 2022, the World Organization of Health (WHO) developed the first Fungal Pathogens Priority List (FPPL) [8]. The FPPL focuses on fungal pathogens that cause invasive and acute and subacute systemic fungal infections for different resistance profiles. The pathogens were ranked in three groups: critical, high and medium. There are five *Candida* spp. included in these groups. *Candida albicans* (*C. albicans*) is the most common pathogenic *Candida* species in humans, responsible for both debilitating mucosal infections and life-threatening systemic infections [9,10], however, the proportion of candidemia cases caused by non-albicans *Candida* (NAC) species is increasing worldwide [7]. Among the NAC species, *Candida glabrata (C. glabrata)* has emerged as an important pathogen due to its increasing incidence in invasive candidiasis and is associated with high mortality rates [11,12].

C. glabrata, now classified as *Nakaseomyces glabratus* [13], leads the high priority group and is the second most prevalent *Candida* spp. yeast pathogen in humans just after *C. albicans.* Although *C. glabrata* is a natural commensal yeast in the

human gut, genitourinary tract, and oral cavity, its incidence as an opportunistic pathogen has increased in the last two decades [14]; causing bloodstream infections (candidemia) with high mortality rates in immunocompromised patients. This pathogen exhibits innately low susceptibility to azole drugs, especially fluconazole [6,10,15]. Furthermore, some studies have found resistance to the echinocandin class of antifungals among already azole-resistant *C. glabrata* clinical isolates [16].

In routine clinical practice, blood cultures remain the gold standard method for detecting *C. glabrata*. Upon pathogen identification, standard protocols usually characterize a single colony (referred to as the index strain). In the context of host-pathogen interactions, two main hypotheses describe infection dynamics: the Independent Action Hypothesis (IAH) and the Cooperative Hypothesis [17]. The IAH proposes that pathogenic organisms act individually, each with its own probability of causing systemic infection assuming a phenotypically and genotypically identical population. Conversely, the Cooperative Hypothesis suggests that pathogens can act collectively, enhancing their persistence and virulence through cooperative mechanisms. Most of the healthcare centers align with the IAH [18,19].

Currently, there are limited therapeutic options to treat fungal infections, primarily restricted to azoles, polyenes, and echinocandins, and their effectiveness can be reduced due to delayed diagnosis or the increasing emergence of antifungal resistance which may develop during treatment [20]. This resistance is still not fully understood, nor is the genetic diversity of the pathogens infecting a single patient. In this context, analyzing isolates collected sequentially during infection has helped to identify genetic or physiological changes that are important for better understanding disease progression and treatment outcomes [21].

Moreover, genetic and phenotypic variation mechanisms are essential for generating diversity within species. At the phenotypic level, gene expression, epigenetic regulation, environmental factors, and biological noise all contribute to variation in observable traits [17,19,22]. Physical, biochemical, and morphological traits can vary significantly depending on environmental conditions and the genetic regulation of each organism. These phenomena are crucial for the adaptation and survival of different populations within their hosts [9,15,16,18].

In this context, recent studies have demonstrated that, in certain cases, contemporaneous clonal strains already display genotypic and phenotypic differences at the time of candidemia diagnosis. These contemporaneous strains have been studied through the isolation and characterization of multiple colonies derived from the initial culture of the same sample, revealing the presence of both genotypic and phenotypic differences among them [18,23].This may lead to an underestimation of intra-patient variability, and undetected antifungal resistance has been reported when the IAH is assumed [23]. This has been demonstrated in studies using contemporaneous isolates, defined as multiple index strains obtained either at the onset or during later stages of infection but from the same sample and at the same time, which allows the assessment of the genetic and phenotypic diversity present from the early stages of infection [5,23]. In this regard, the accurate diagnosis of *C. glabrata* is essential for an appropriate antifungal therapy, since each clinical isolate may exhibit different susceptibility profiles to different stressors, including temperature and antifungal agents.

This study aimed to identify and characterize 8 contemporaneous strains of *C. glabrata* obtained from three different patients. We obtained a total of 40 contemporaneous isolates from Patient 6 (P6), Patient 8 (P8), and Patient 10 (P10). Genotyping analyses suggest that the contemporaneous strains from each patient shared a clonal origin, as determined by MLP analysis and the *EPA1* marker. No phenotypic variation under different stress conditions was observed among the P8 isolates; however, phenotypic differences were detected in contemporaneous isolates from P6 and P10.

In P10 isolates, differences in growth on non-fermentable carbon sources (YPG) were observed compared with the expected phenotype on fermentable media. Therefore, additional growth assays were performed using another non-fermentable carbon source and under tetrazolium chloride (TTC) stress conditions. TTC medium was used as an indicator of respiratory chain activity through TTC reduction. No evidence of mitochondrial dysfunction was detected, since the isolates were able to grow on glycerol and ethanol as non-fermentable carbon source (Gly+) and were also capable of reducing TTC, producing a pink coloration.

Phenotypic assays revealed that contemporaneous isolates from P6 exhibited differential responses under high concentrations of fluconazole (FLC). Consequently, Minimum Inhibitory Concentration 50 (MIC_{50}) assays were performed using two methodologies and three antifungal agents belonging to two different classes, azoles and echinocandins, including FLC (azole), caspofungin (CSP), and micafungin (MICA) (echinocandins). No significant differences were detected among the P6 contemporaneous isolates in the MIC_{50} assays for FLC, CSP, and MICA. However, slight differences in the doubling times during growth in the presence of FLC were found among the P6 isolates.

Taken together and supported by previous work from our research group (Aranda Moreno et al. (2025) master's thesis), our findings suggest the early emergence of phenotypic variability among contemporaneous isolates of *C. glabrata* from P6. This variability may contribute to an underestimation of antifungal interactions in clinical settings, potentially leading to ineffective treatment during infection and to the subsequent acquisition of resistance against first-line antifungal agents, such as azoles and echinocandins.

2. Results

2.1. Isolation of 40 contemporaneous clinical strains from *C. glabrata* isolates from three patients.

The classical model of infections proposes that most bloodstream infections, including candidemia, are caused by genetically identical populations derived from a single organism that successfully passes through the infection bottleneck. Consequently, most studies addressing *Candida* diversity have focused on longitudinal isolates rather than contemporaneous isolates [23].

In this study, we aimed to identify and characterize contemporaneous strains of *C. glabrata* obtained from blood samples from three different patients (Table 1).

Table 1. *C. glabrata* clinical isolates collection chosen for this work from different patients in our laboratory's existing collection.

Lab patient No	Hospital patient No	Sample No	Date	Lab collection No	Sampling site
Patient 6 (P6)	271673	14019522	16-mar-14	AN264	No data available
		14019523	16-mar-14	AN359	No data available
Patient 8 (P8)	61094	16012786	20-feb-16	AN506	Catheter
		16012787	20-feb-16	AN505	Right arm
		16012788	20-feb-16	AN483	Left arm
Patient 10 (P10)	294172	18031203	04-may-18	AN755	Left arm
		18031204	04-may-18	AN756	Medial catheter
		18031205	04-may-18	AN757	Proximal catheter

As a result, a new collection composed of five contemporaneous strains derived from each selected isolate was generated. We selected contemporaneous isolates from Patient 6 (P6), Patient 8 (P8), and Patient 10 (P10). In total, we obtained 10 new

isolates from P6, 15 from P8, and 15 from P10, resulting in 40 new contemporaneous isolates overall. All contemporaneous strains were incorporated into the collection of the Molecular Microbiology of Fungi Laboratory, DBM, IPICYT (Fig. 1.).

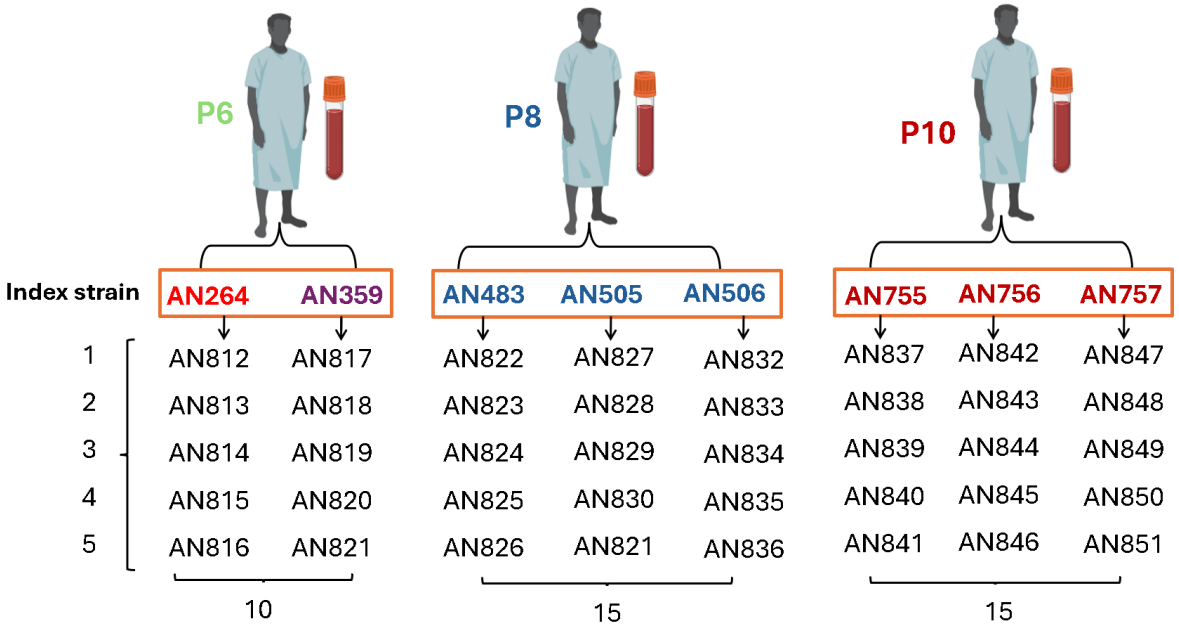

Fig. 1. *C. glabrata* contemporaneous strains obtained from P6, P8 and P10.
A total of 40 contemporaneous isolates were obtained from parental clinical isolates of C. *glabrata* derived from Patient 6 (P6), Patient 8 (P8), and Patient 10 (P10). The contemporaneous isolates enclosed within the orange box are contemporaneous to each other and served as the index strains for each contemporaneous isolate set.

2.2. *C. glabrata* contemporaneous clinical strains likely share a clonal origin in each patient

To rule out the possibility that the clinical samples, contemporaneous isolates among themselves, originated from mixed candidemia, it was essential to confirm that the contemporaneous isolates shared a common clonal origin. To address this, we performed genotyping analyses using the microsatellite length polymorphisms (MLP) technique.

A total of 40 contemporaneous strains were genotyped using three primer sets directed against the molecular markers *RPM2*, *MT-I,* and *ERG3*, amplifying microsatellite regions through MLP analysis (Table 2) [24]. These markers have

been shown to be highly discriminatory, reproducible, and stable across multiple generations, making them effective for strain identification [25].

Table 2. List of primer sequences used to identify and genotype contemporaneous clinical isolates

Primer	Secuence 5´- 3´	Expected size (bp)
EPA1	Fw**.** CGACTTCAATGCTACTTCCTCCG	800-1000bp
	Rv**.** GGGTGCTATGTACCTTGCGACATG	
ERG3	Fw. AGTGCGAGTGTATGTAAAGAATG	Chromosome F (181-353bp)
	Rv. CGTATACCTTATCTCCGTTCAA	
MT-I	Fw. AGCAATAATAGCTTCTGACTATGAC	Chromosome D (227-251bp)
	Rv. GACAGGAGCAACCGTTAGGA	
RPM2	Fw. ATCTCCCAACTTCTCGTAGCC	Chromosome I (116-150bp)
	Rv. ACTTGAACGACTTGAACGCC	

Fw= Forward; Rv= Reverse.

After determining the relative migration distances of PCR products on 2% agarose gels using ImageJ© for each contemporaneous group from each patient (S1-3 Figs), no differences were detected among the alleles of the contemporaneous *C. glabrata* isolates in any of the patients. Using the ImageJ© data obtained for each marker and patient, a dendrogram was generated with the *hclust* function in the R programming language© (Fig. 2.).

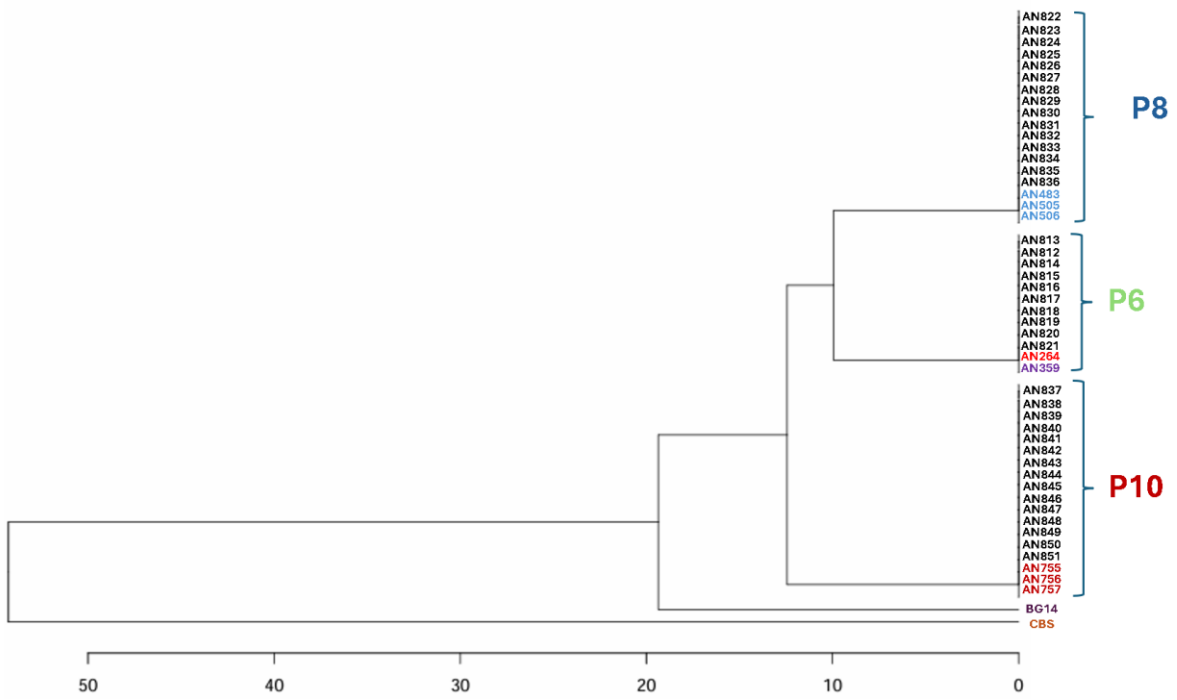

Fig. 2. Dendrogram of *C. glabrata* contemporaneous strains from P6, P8 and P10 by MLP markers. The contemporaneous strains from P6, P8 and P10 share a clonal origin because they were clustered together and separately from the reference strains. ImageJ® and RStudio® were used to construct the dendrogram based on the sizes of PCR products obtained with each of the three molecular markers (*MT-I*, *ERG3* and *RPM2*).

To further confirm the clonal origin of the isolates from each patient, we also analyzed the tandem repeat region located within the ORF of the *EPA1* gene. Variability in the number of tandem repeats within this linker domain has previously been identified among clinical isolates [26]. However, amplification of *EPA1* showed no differences in the PCR products among isolates from the same patient (Fig. 3.). Together, these results suggest that the contemporaneous strains from P6, P8, and P10 originated from the same clonal population in each patient, since they consistently clustered together and independently from the reference strains.

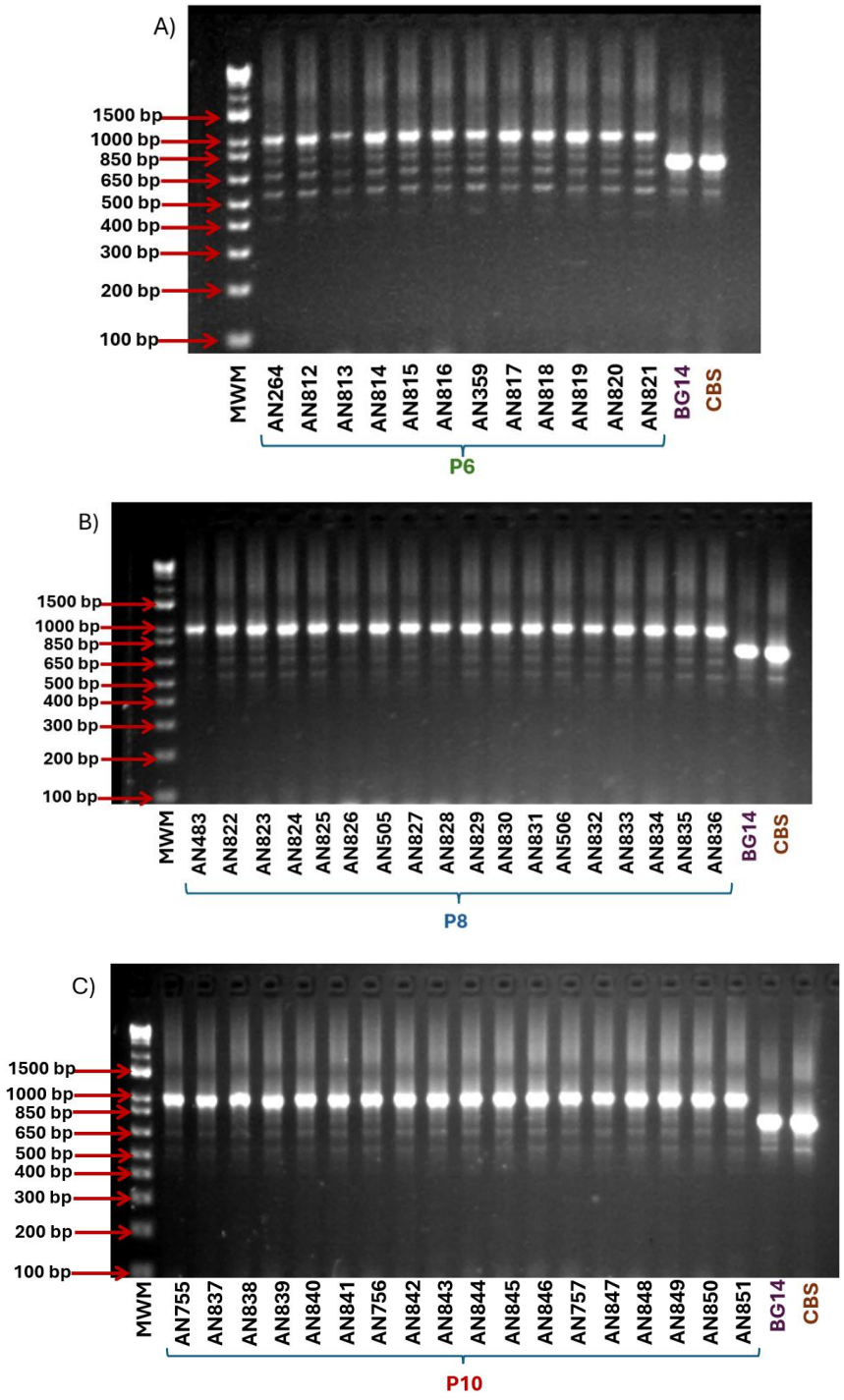

Fig. 3. *EPA1* microsatellites of contemporaneous isolates.

The contemporaneous isolates from P6 (A), P8 (B), and P10 (C) exhibited the same banding pattern for the microsatellite regions of *EPA1* within the ORF amplified by PCR, and clustered independently from the reference strains.

2.3. Contemporaneous strains from P6 and P10 display phenotypic variability

Pathogen microevolution within the host has not been analyzed extensively in contemporaneous strains, in this work, we analyzed whether our collection of contemporaneous strains exhibited differences in their capacity to respond to environmental and antifungal stresses within each patient group using spot-growth assays performed under multiple stress conditions. We evaluated susceptibility profiles associated with cell wall and membrane stress, thermal stress, oxidative stress, mitochondrial function, and antifungal exposure (S4 Fig.). Overall, no major growth differences were observed among the contemporaneous groups from any patient under the tested conditions (Table 3).

Table 3. Susceptibility assays in *C. glabrata* contemporaneous strains obtained from P6, P8 and P10

Patient	Clinical sample	Contemp. strain	Susceptibility assay																
			Heat shock		Non ferment. carbon source		Cell wall and membrane stressors				Oxidative stress		Antifungals						
			YPD, (°C)		YPG (°C)		SDS %, 30°C		Caffeine [mM], 30°C		H_2O_2 [mM], 30°C		FLC [µg/ml], 30°C				CSP [µg/ml], 30°C		
			37	45	30	37	0.075	0.1	0.075	0.1	10	15	8	16	20	32	0.035	0.05	0.07
P6	AN 264	AN812	R	S	R	R	R	R	R	S	R	R	R	R	R	R	R	R	S
		AN813	R	S	R	R	R	R	R	S	R	R	R	R	R	R	R	R	S
		AN814	R	S	R	R	R	R	R	S	R	R	R	R	R	R	R	R	S
		AN815	R	S	R	R	R	R	R	S	R	R	R	R	R	R	R	R	S
		AN816	R	S	R	R	R	R	R	S	R	R	R	R	R	R	R	R	S
	AN 359	AN817	R	S	R	R	R	R	R	S	R	R	R	R	R	R	R	R	S
		AN818	R	S	R	R	R	R	R	S	R	R	R	R	R	R	R	R	S
		AN819	R	S	R	R	R	R	R	S	R	R	R	R	R	R	R	R	S
		AN820	R	S	R	R	R	R	R	S	R	R	R	R	R	R	R	R	S
		AN821	R	S	R	R	R	R	R	S	R	R	R	R	R	R	R	R	S

P8	AN 483	AN822	R	S	R	R	R	R	R	S	R	R	R	S	S	S	R	R	S
		AN823	R	S	R	R	R	R	R	S	R	R	R	S	S	S	R	R	S
		AN824	R	S	R	R	R	R	R	S	R	R	R	S	S	S	R	R	S
		AN825	R	S	R	R	R	R	R	S	R	R	R	S	S	S	R	R	S
		AN826	R	S	R	R	R	R	R	S	R	R	R	S	S	S	R	R	S
	AN 505	AN827	R	S	R	R	R	R	R	S	R	R	R	S	S	S	R	R	S
		AN828	R	S	R	R	R	R	R	S	R	R	R	S	S	S	R	R	S
		AN829	R	S	R	R	R	R	R	S	R	R	R	S	S	S	R	R	S
		AN830	R	S	R	R	R	R	R	S	R	R	R	S	S	S	R	R	S
		AN831	R	S	R	R	R	R	R	S	R	R	R	S	S	S	R	R	S
	AN 506	AN832	R	S	R	R	R	R	R	S	R	R	R	S	S	S	R	R	S
		AN833	R	S	R	R	R	R	R	S	R	R	R	S	S	S	R	R	S
		AN834	R	S	R	R	R	R	R	S	R	R	R	S	S	S	R	R	S
		AN835	R	S	R	R	R	R	R	S	R	R	R	S	S	S	R	R	S
		AN836	R	S	R	R	R	R	R	S	R	R	R	S	S	S	R	R	S
P10	AN 755	AN837	R	S	R	R	R	R	R	S	R	R	R	R	R	S	R	S	S
		AN838	R	S	R	R	R	R	R	S	R	R	R	R	R	S	R	S	S
		AN839	R	S	R	R	R	R	R	S	R	R	R	R	R	S	R	S	S
		AN840	R	S	R	R	R	R	R	S	R	R	R	R	R	S	R	S	S
		AN841	R	S	R	R	R	R	R	S	R	R	R	R	R	S	R	S	S
	AN 756	AN842	R	S	R	R	R	R	R	S	R	R	R	R	R	S	R	S	S
		AN843	R	S	R	R	R	R	R	S	R	R	R	R	R	S	R	S	S
		AN844	R	S	R	R	R	R	R	S	R	R	R	R	R	S	R	S	S
		AN845	R	S	R	R	R	R	R	S	R	R	R	R	R	S	R	S	S
		AN846	R	S	R	R	R	R	R	S	R	R	R	R	R	S	R	S	S
	AN 757	AN847	R	S	R	R	R	R	R	S	R	R	R	R	R	S	R	S	S
		AN848	R	S	R	R	R	R	R	S	R	R	R	R	R	S	R	S	S
		AN849	R	S	R	R	R	R	R	S	R	R	R	R	R	S	R	S	S
		AN850	R	S	R	R	R	R	R	S	R	R	R	R	R	S	R	S	S

		AN851	R	S	R	R	R	R	R	S	R	R	R	R	R	S	R	S	S

Contemporaneous isolates that exhibited resistance to stress (R) are indicated with a purple background; these correspond to isolates that growth in the single-drop assay. Contemporaneous isolates that exhibited susceptibility to stress (S) are indicated with a pink background; these correspond to isolates that did not grow in the single-drop assay.

However, the entire P10 contemporaneous group exhibited reduced growth on YPG medium at 30°C compared with growth under standard YPD conditions (Fig. 4.). This phenotype suggested a possible mitochondrial dysfunction, since impaired mitochondrial activity compromises the utilization of alternative non-fermentable carbon sources such as glycerol, thereby limiting cellular growth under these conditions.

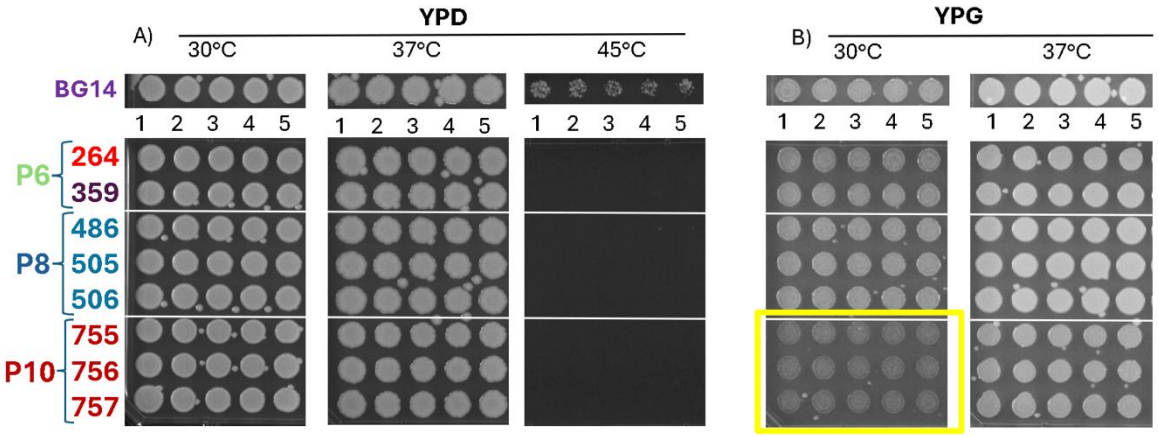

Fig. 4. Phenotypic characterization of contemporaneous *Candida glabrata* isolates by drop-spot assay. (A) Growth of contemporaneous isolates from P6, P8 and P10 on YPD medium under different temperature conditions. (B) Growth of the same isolates on YPG medium as a non-fermentable carbon source stress condition at different temperatures. The yellow box highlights the reduced growth phenotype observed in the P10 contemporaneous isolates on YPG medium at 30°C.

In contrast, differences in growth under fluconazole stress (20µg/mL) were observed among the P6 isolates between the two contemporaneous sets that make up the patient group (Fig. 5). These findings suggested potential variability in antifungal

response among contemporaneous isolates, particularly against fungistatic agents such as fluconazole.

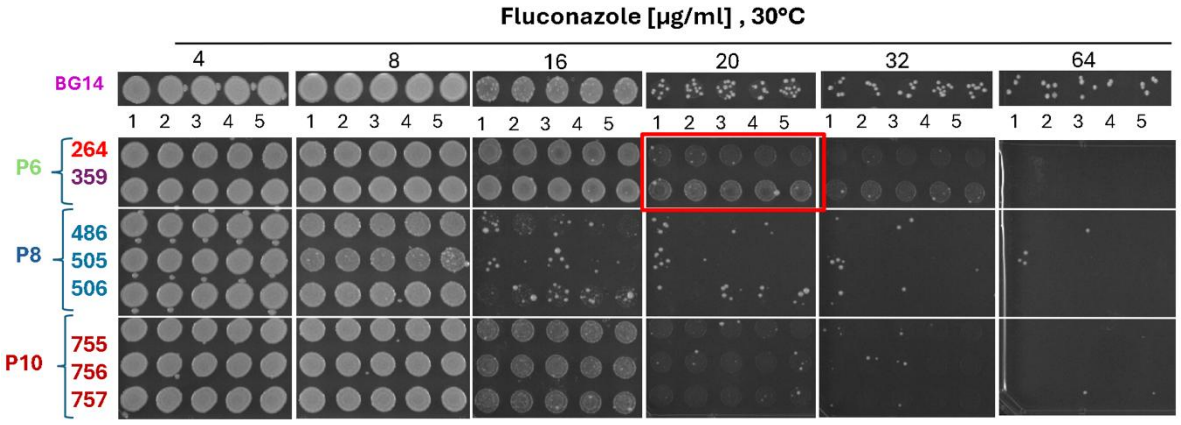

Fig. 5. Drop-spot assay of contemporaneous *Candida glabrata* isolates under FLC stress. Growth of all contemporaneous isolates was evaluated in the presence of increasing concentrations of FLC. The red box highlights the isolates from P6, where differences in growth were observed between the two contemporaneous isolate sets, suggesting variability in the response to fluconazole stress.

2.4. P10 isolates maintained functional mitochondrial respiratory activity

Functional mitochondria is essential for the utilization of non-fermentable carbon sources such as acetate, lactate, fatty acids, ethanol, glycerol and oleate [27].

Respiratory-deficient "*petite*" mutants of *C. glabrata* have been characterized by their inability to grow on glycerol as the carbon source (Gly-), and mitochondrial dysfunction frequently leads to the petite Gly- phenotype.

To study this phenotype, the compound 2,3,5-triphenyltetrazolium chloride (TTC) is used, because it is a colorless electron acceptor that is reduced under reductive conditions to form a red formazan product in yeasts that have functional mitochondria. For this reason, TTC is employed as a qualitative screening method to determine dysfunctional respiratory chain.

We tested the ability of contemporaneous isolates to reduce TTC by spot growth assay and observed that the P10 isolates formed pink colonies indicating TTC reduction. This suggests that mitochondria in P10 strains are functional. As controls, we used laboratory reference strains BG14 and CBS, which display a normal growth phenotype on non-fermentable carbon sources and BrEt-derived petite strains

CGM1938 and CGM1939, which are unable to grow on non-fermentable carbon sources and form white colonies (S1 Table). P10 contemporaneous isolates were able to grow on both YPG and YPE media and displayed pink coloration in the TTC assay (Fig. 6). These results indicate that the P10 isolates maintain functional mitochondrial respiratory activity despite the slow growth initially observed during phenotypic characterization assays.

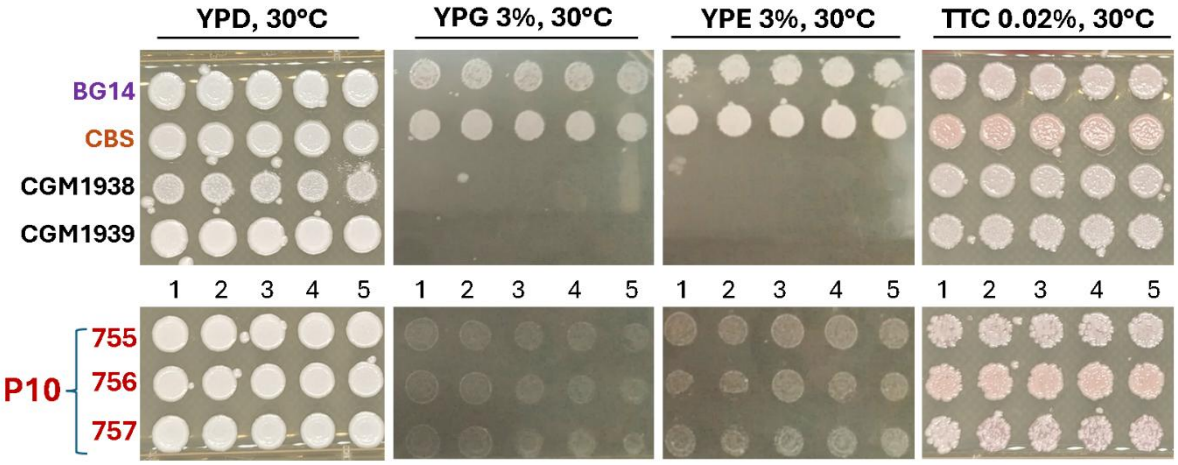

Fig 6. Mitochondrial function in contemporaneous isolates from P10. Drop-spot assays were performed on YPD medium as a control, YPG and YPE media as non-fermentable carbon source conditions, and TTC medium as an indicator of respiratory chain activity through TTC reduction. Compared to the reference petite strains, CGM1938 and CGM1939, the P10 contemporaneous isolates did not exhibit a mitochondrial dysfunction phenotype. Notably, all P10 isolates were able to grow on YPG and YPE media and developed the characteristic pink coloration in the TTC assay, indicating preserved mitochondrial respiratory activity.

2.5. Contemporaneous isolates from P6 displayed similar MIC_{50} for FLC, CSP and MICA

The MIC represents the lowest concentration of an antifungal drug capable of inhibiting visible fungal growth. MIC_{50} refers to the drug concentration that inhibits the growth in the 50% of the population of a strain and is therefore used as a measure of the typical susceptibility profile of a microbial population rather than of an individual clinical isolate [28]. In clinical practice, MIC_{50} values are mainly useful

for understanding population susceptibility trends, guiding the antifungal selection, monitoring resistance and supporting the establishment of clinical breakpoints and epidemiological cutoff values (ECVs) [29].

Currently, two major independent standards are used for antifungal susceptibility testing in *Candida* spp: the broth microdilution (BMD) method developed by the CLSI and the BMD method established by the EUCAST [30]. Although CLSI and EUCAST use different technical methodologies and interpretive criteria, both systems aim to classify *C. glabrata* isolates similarly as susceptible or resistant [31]. For most antifungal agents, MIC distributions and resulting breakpoints are broadly comparable between the two systems[32,30].

To evaluate the differences in growth among the P6 contemporaneous isolates in the presence of antifungal agents, we first analyzed their growth in liquid YPD medium under non-stress conditions for 25 hours using the BMD method by CLSI. Additionally, using the same methodology, we determined the MIC_{50} for FLC for each contemporaneous isolate. First, growth curve analyses under non-stress conditions (no antifungal) demonstrated that isolates derived from the parental isolate AN264 (from P6) displayed similar growth rates among all contemporaneous isolates and the parental strain itself. Likewise, isolates derived from the parental isolate AN359 exhibited comparable growth rates among all contemporaneous isolates and their corresponding parental strain (Fig. 7.).

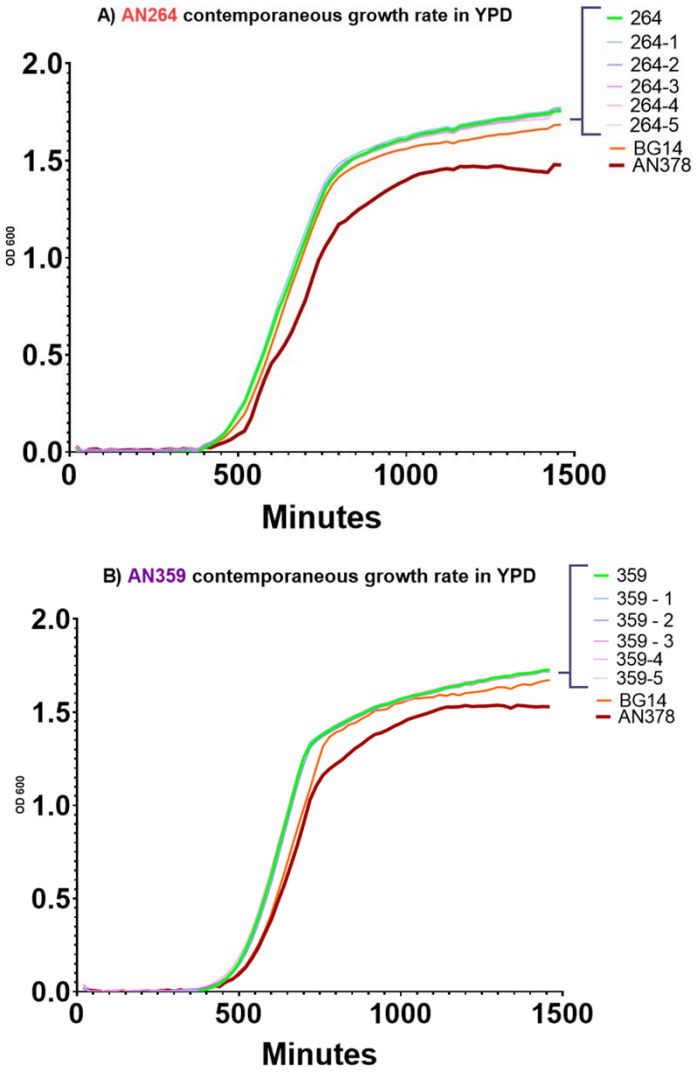

Fig 7. Growth curves of contemporaneous *C. glabrata* strains from P6 evaluated by AUC method under non-stress conditions. (A) Growth curves over 25 hours in YPD medium of contemporaneous isolates derived from parental isolate AN264, including the parental strain and two laboratory reference strains, BG14 (susceptible dose dependent to FLC) and AN378 (FLC^R). (B) Growth curves over 25 hours in YPD medium of contemporaneous isolates derived from parental isolate AN359, including the parental strain and two laboratory reference strains. In both groups, contemporaneous isolates exhibited growth curves comparable to their corresponding parental isolate, indicating similar growth dynamics under non-stress conditions. (AN812 = 264-1, AN813 = 264-2, AN814 = 264-3, AN815 = 264-4, AN816 =264-5; AN817= 359-1, AN818 = 359-2, AN819 = 359-3, AN820 = 359-4 and AN821 = 359-5).

The MIC_{50} values obtained for FLC also showed similar growth behavior among isolates derived from AN264, and the same pattern was observed for isolates derived from AN359 (Table 4).

Table 4. MIC_{50} values obtained by AUC analysis for contemporaneous *C. glabrata* strains from P6 under FLC stress condition in YPD medium.

	Isolate	MIC_{50}(µg/m) ± SD
Contemporaneous strains	AN264	8.6 ± 0.9
	AN264-1	8.7 ± 0.9
	AN264-2	7.8 ± 0.2
	AN264-3	8.4 ±1.1
	AN264-4	8.3 ±1.8
	AN264-5	7.4 ± 3.1
	AN359	7.8 ± 1.0
	AN359-1	8.0 ± 1.0
	AN359-2	8.2 ± 0.9
	AN359-3	7.8 ±1.4
	AN359-4	8.2 ±1.1
	AN359-5	7.6 ± 1.1
Controls	AN378	57.3 ± 8
	BG14	11.6 ± 0.2

(BG14 = FLC^{SDD}).

FLC^{SDD}→ ≤32 µg/ml; FLC^{R} →≥64 µg/ml;

However, when comparing the growth curves of the parental isolates AN264 and AN359 in the presence of 16µg/ml of FLC, we observed that, although not statistically significant, AN264 has a decreased slope compared to AN359 (Fig. 8.) which results in a longer doubling time for AN264 only in the presence of FLC but not under non-stress conditions or in the presence of FLC at concentrations close to the MIC_{50} (Table 5).

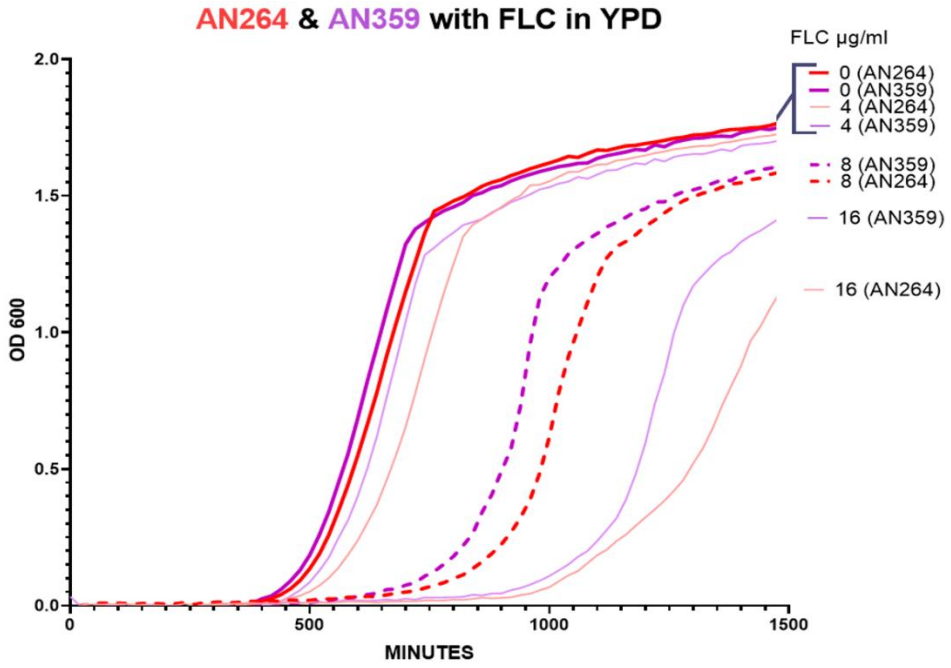

Fig. 8. Growth kinetics of the parental isolates AN264 and AN359 under FLC stress conditions

Growth curves over 25 hours in YPD medium of parental isolate AN264 (red) and parental isolate AN359 (purple) are shown under different FLC concentrations. Dashed lines indicate the growth values closest to the MIC_{50} obtained for each parental isolate. Although no significant differences in growth were observed among the contemporaneous isolates, AN359 displayed a shorter lag phase than AN264 in the presence of fluconazole in the MIC_{50} concentration.

Table 5. Doubling times of P6 index strains in the presence of FLC in YPD medium.

		Doubling time (minutes)		
		AN264	**AN359**	**BG14**
FLC (µg/ml)	**0**	52.3 ± 0.8	51.6 ± 2.3	50.3 ± 2.3
	8	75.9 ± 2.0	71.2 ± 2.3	61.9 ± 4.9
	16	107.3 ± 10.7	83.9 ± 4.3	65.0 ± 3.0

After characterizing the overall growth behavior of the contemporaneous groups, we selected two representative contemporaneous isolates derived from each parental isolate to further evaluate their interaction with three of the most commonly used

antifungal agents in clinical settings. MIC_{50} assays were performed following the BMD by EUCAST protocol for FLC, CSP, and MICA in Roswell Park Memorial Institute (RPMI) medium.

MIC_{50} values were determined for the selected contemporaneous isolates as well as for the laboratory reference strains for each of the three antifungal agents. The results again demonstrated that no significant differences in growth were observed among the contemporaneous isolates groups in response to the fungicidal agents CSP and MICA or the fungistatic agent FLC (Table 6).

Table 6. MIC_{50} values determined by the EUCAST protocol for representative contemporaneous *C. glabrata* strains from P6 against FLC, CSP and MICA in RPMI medium.

	Isolate	MIC_{50}(µg/ml) ± SD		
		FLC	CSP	MICA
Contemporaneous strain	AN264	6.6 ± 1.79	0.073 ± 0.003	0.075 ± 0.0009
	AN264-1	9.4 ± 0.32	0.071 ± 0.002	0.072 ± 0.001
	AN264-2	8.6 ± 0.2	0.072 ± 0.003	0.071 ± 0.002
	AN359	6.5 ± 0.87	0.073 ± 0.004	0.073 ± 0.001
	AN359-1	8.9 ± 0.06	0.073 ± 0.002	0.073 ± 0.001
	AN359-2	8.2 ± 0.27	0.072 ± 0.004	0.072 ± 0.002
Controls	AN376	N/D*	0.657 ± 0.03	0.064 ± 0.001
	AN378	37.7 ± 1.52	N/D*	0.070 ± 0.001
	BG14	9.5 ± 0.33	0.071 ± 0.001	0.071 ± 0.001

(AN812 = 264-1, AN813 = 264-2, AN817 = 359-1, and AN818 = 359-2).

FLC^R →≥16 µg/ml (BMD by EUCAST method). CSP^R→≥0.5 µg/ml, $MICA^R$→≥0.25µg/ml (BMD by CLSI method). N/D*= Not determined

3. Discussion

3.1. Clinical contemporaneous strains share a clonal origin among patients and no major phenotypic variability was found

The prevalence of *C. glabrata* as a causative agent of bloodstream infection (BSI), or candidemia, has been associated not only with previous exposure to fluconazole, but also with factors such as geographic location, age, and other characteristics of the studied population [7]. One study identified independent factors associated with an increased risk of *Candida* BSI, including previous surgery, acute renal failure, use of parenteral nutrition, and, in surgical patients, the presence of a catheter [33]. For this reasons, there is a possibility that BSIs may result from mixed fungemias [34].The results of this study revealed that contemporaneous isolates of *C. glabrata* obtained from different blood samples but at the same point in time, share a clonal origin but may present phenotypic differences from the early stages of infection, because we observed variability in growth of P10 clinical contemporaneous isolates sets at 30°C in YPG, which suggests a possible dysfunction at mitochondrial level. Moreover, the sets of P6 clinical contemporaneous isolates displayed growth differences under FLC stress. This is consistent with recent reports that demonstrated that during candidemia, fungal populations are not necessarily completely homogeneous, even when they originate from the same infectious event [5,23].This is relevant because *C. glabrata* possesses a high adaptive capacity under adverse conditions, including oxidative stress, temperature changes, and antifungal exposure, characteristics that contribute to its success as an opportunistic pathogen [11,21,27].

3.2. Contemporaneous P10 strains do not display mitochondrial disfunction

Isolates from P10 initially showed a lower growth in YPG at 30° C compared to 37°C. This phenotype is strongly associated with metabolic alterations and increased resistance to azole antifungals because loss of mitochondrial function correlates with azole resistance [35]. Similarly, clinical azole resistant isolates of *C. glabrata* have shown reduced ATP production and oxygen consumption, with several strains exhibiting a Gly- phenotype indicative of respiratory deficiency [36].

In *Saccharomyces cerevisiae*, TTC reduction is associated to the mitochondrial respiratory activity of ubiquinol-cytochrome *c* oxidoreductase (complex III), rather

than cytochrome *c* oxidase [37]. Likewise, in *Candida albicans*, TTC reduction has been associated with mitochondria-like particulate structures, further supporting its use as a marker of mitochondrial respiratory activity [38].

Because TTC reduction depends on respiratory-chain dehydrogenases and yeast mitochondrial activity, its application in *C. glabrata* as a marker of functional versus defective respiration is well supported. However, interpretation of the assay requires caution, as TTC reflects overall electron flow rather than the activity of a single respiratory complex [37,39]. Furthermore, TTC is reduced mainly by proximal respiratory complexes (I/III), and the resulting formazan product is unstable in the presence of oxygen. Consequently, the assay distinguishes only certain classes of mitochondrial defects and requires strict control of experimental conditions for interpretation [37–39].

In this study, phenotypic assays in YPE and TTC demonstrated that the contemporaneous isolates from P10 maintain functional respiratory activity, as they are able to grow on non-fermentable carbon sources and reduce TTC. This indicates that the observed phenotype most likely corresponds to more subtle metabolic adjustments rather than severe mitochondrial dysfunction.

3.3 Contemporaneous clinical strains from P6 do not show differences in growth under different antifungals stress

In *C. glabrata*, MIC_{50} values for FLC, CSP, MICA and other types of drugs provide important information regarding the overall susceptibility of local or regional isolate populations [28]. When interpreted together with the full MIC range, MIC_{50} data also help to identify shifts in susceptibility distributions and the emergence of subpopulations with elevated MICs that may indicate developing antifungal resistance [28,40]. Knowing local MIC_{50} values and resistance frequencies in an infection by *C. glabrata* can help determine whether FLC remains an appropriate option or whether initial therapy with an echinocandin such as CSP or MICA is preferable [32,41]. Here, the contemporaneous isolates from P6 showed differences in growth under FLC stress during spot dilution assays. In addition, MIC_{50} analyses and growth curves demonstrated similar susceptibility profiles among the isolates. However, slight differences in the growth rate between AN264 and AN359 were observed in the presence of FLC. These results suggest that early adaptive

responses to antifungal stress may exist even within clonal populations. Recent studies have proposed that phenotypic heterogeneity may represent early stages of antifungal adaptation before the acquisition of stable resistance [18,23].

The MIC_{50} values obtained for FLC, CSP, and MICA remained within comparable ranges among contemporaneous isolates, indicating that there are no major differences in antifungal susceptibility within each clonal group. This is relevant considering that azoles and echinocandins continue to be first-line therapy against invasive *C. glabrata* infections [32,41].

7.1. Clinical implications of the phenotypic characterization of multiple index strains during candidemia

Overall, the results obtained, together with previous work from our research group (Aranda Moreno et al. (2025) master's thesis), support the idea that contemporaneous populations of *C. glabrata* derived from the same clinical sample share a clonal origin while developing phenotypic variations. These differences could represent early adaptive events during infection and highlight the importance of studying multiple colonies obtained from the same clinical sample to avoid underestimating the phenotypic variation present during candidemia (Fig. 9). This could contribute to a more accurate clinical diagnosis and, consequently, the selection of appropriate therapeutic strategies for patient treatment.

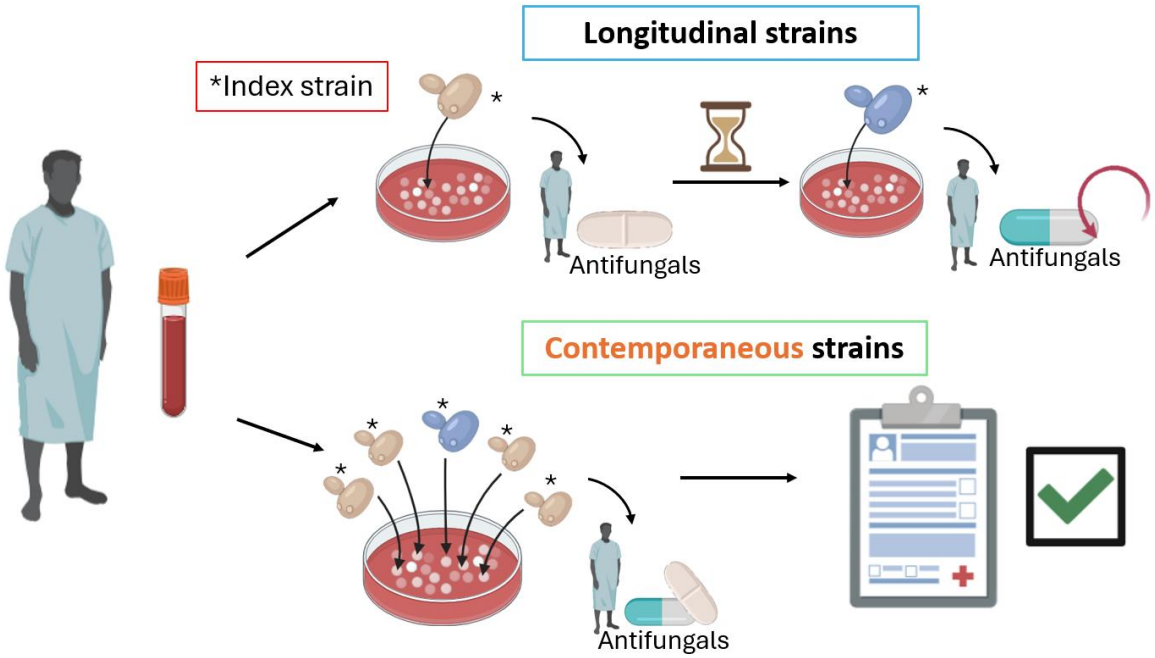

Fig. 9. Phenotypic variability may be underestimated in clinical practice.
In clinical practice, the timely diagnosis of *C. glabrata* is important for determining susceptibility to different antifungal agents to provide appropriate treatment. In hospital laboratories, once the etiological agent causing the disease has been identified, the characterization of a single isolate, known as the index strain (red box), is usually performed, since it is generally assumed that identical morphotypes do not exhibit phenotypic variability at the time of identification. After the diagnosis of the index strain, an appropriate treatment for the patient is established. Throughout the candidemia episode, additional index strains may continue to be characterized to identify possible variability and determine whether acquired resistance to different antifungal agents has developed. These are known as longitudinal strains (blue box). However, recent studies have shown that such variability may already be present from the initial diagnosis of the patient. Therefore, limiting the analysis to a single index strain could lead to an underestimation of antifungal susceptibility. By analyzing more than one index strain at the time of diagnosis, the likelihood of selecting an appropriate treatment increase. When multiple index strains are simultaneously characterized at the same time point, they are referred to as contemporaneous strains (green box).

Materials and methods

1. *C. glabrata* strains

The reference strains from the Molecular Microbiology Laboratory, DBM, IPICYT used in this study were strain BG14 and strain CBS138 (CBS) as identification controls for the genotyping of contemporaneous clinical isolates of *C. glabrata* using 3 primer sets of the molecular markers *ERG3*, *MT-I*, and *RPM2* by microsatellite length polymorphisms (MLP) technique, for the analysis of the tandem repeats region located within the ORF of the *EPA1* gene. Strains CGM1938 and CGM1939 are petite mutants generated with ethidium bromide and were used as growth controls in mitochondrial stress assays with non-fermentable carbon sources. Strains AN376 and AN378 were used as FLC^S, CAS^R and FLC^R, CAS^S controls respectively in MIC_{50} assays.

The strains used are described in S1 Table.

2. Selection of contemporaneous strains from clinical samples

All contemporaneous isolates of *C. glabrata* included in this study were obtained from clinical blood samples provided by the Instituto Nacional de Ciencias Médicas y Nutrición Salvador Zubirán (INCMNSZ) and incorporated into the collection of the Molecular Microbiology Laboratory, DBM, IPICYT (Table 2).

The isolates originated from the initial diagnosis of *C. glabrata*, in which identification and characterization were carried out from a single colony, designated as the index strain. Strains were classified as contemporaneous when they were recovered from the same patient on the same date and assigned consecutive sample numbers.

For propagation, each isolate was cultured in Yeast Peptone Dextrose with 2% of glucose (YPD) liquid medium for two nights at 30°C under controlled conditions. After incubation, cultures were standardized to an OD_{600} of 1 using sterile water. Serial 1:10 dilutions of the cell suspensions were prepared until $1x10^{-5}$ and plated onto YPD solid medium for 48 hours at 30°C. From each index strain, five contemporaneous strains were selected for subsequent analyses.

Single colonies for each selected index strain were streak purified twice and a single isolated colony from each streak was selected and subsequently grown on YPD solid medium for two nights at 30°C. After incubation, five strains derived from each isolate

were retained for additional characterization and incorporated into the laboratory collection.

As a result, a new collection consisting of five contemporaneous strains derived from each selected isolate was established. Contemporaneous isolates from Patient 6 (P6), Patient 8 (P8), and Patient 10 (P10) were selected for this study. In total, 10 new isolates were obtained from P6, 15 from P8, and 15 from P10, resulting in 40 contemporaneous isolates overall. All strains were incorporated into the collection of the Molecular Microbiology of Fungi Laboratory, DBM, IPICYT (samples AN812-AN851).

3. DNA extraction

Genomic DNA from yeast strains was extracted using the FastPrep®-24 (MP Biomedicals) protocol standardized in our laboratory. Each strain was inoculated into 5 mL of YPD broth and incubated at 30°C for 24 hours. Following incubation, cells were harvested by centrifugation and resuspended with 500 µL of buffer A (Tris HCl 50 mM, EDTA 10 mM, NaCl 150 mM, Triton 1%, and SDS 1%) together with 500 µL of phenol:chloroform:isoamyl alcohol. Samples were then processed in the FastPrep system for 1 second at 4 m/s.

After centrifugation, the aqueous phase was recovered and mixed with 15 µL of NaCl 5 M and 1 mL of absolute ethanol. The resulting pellets were washed once using 70% ethanol. Subsequently, 0.2 µL of RNAase cocktail mix (RNase A: 0.1 U/mL and RNase T1: 4 U/mL, Ambion®) was added to each sample, followed by incubation at 37°C for 30 minutes. Finally, DNA samples were resuspended in 200µL of Tris 10mM.

Once genomic DNA was obtained, samples were quantified and subsequently adjusted to a final concentration of 10ng/ml with Tris 10mM for each sample. Genomic DNA was stored at -20°C until further use.

4. Genotyping of *C. glabrata* contemporaneous strains by MLP and *EPA1* microsatellites

To evaluate whether the previously identified clinical isolates of *C. glabrata* shared a common clonal origin, endpoint PCR assays were performed using three primer sets targeting the molecular markers *RPM2*, *MT-I*, and *ERG3*. These assays

amplified microsatellite regions using a modified microsatellite length polymorphisms (MLP) approach.

PCR conditions were established according to the protocol described in López Marmolejo et al. (2021) master's thesis. Reactions were carried out using homemade DNA polymerase in a final reaction volume of 20µL. For electrophoretic analysis, 10µL of each PCR product was loaded onto a 2% agarose gel. PCR product sizes were determined using ImageJ© software, and a dendrogram was generated using the *hclust* function in the R programming language through RStudio©.

Microsatellite regions of *EPA1* within the ORF were amplified by PCR. Reaction conditions were established according to Herrera Basurto et al. (2020) and the manufacturer's instructions for DreamTaq Green Polymerase® (Thermo Fisher Scientific). Each reaction was prepared in a final volume of 5µL, and the complete reaction products were analyzed by electrophoresis on a 2.0% agarose gel.

The primers used for genotyping are shown in Table 3.

5. Phenotypic characterization of *C. glabrata* contemporaneous strains

To evaluate whether contemporaneous strains exhibited differences in their ability to respond to environmental and antifungal stresses within each patient group, we performed spot-growth assays under multiple stress conditions.

Each contemporaneous isolate was inoculated into YPD broth and incubated for 48 hours at 30°C with shaking. After incubation, cultures were adjusted to an OD_{600} of 0.05 using sterile water and subjected to spot-growth assays under different stress and drug susceptibility conditions. Growth on YPD plates at 30°C was used as the control condition, while growth at 37°C and 45°C was evaluated as thermal stress. We also assessed growth on YPG medium containing 3% glycerol instead of dextrose as a non-fermentable carbon source at both 30°C and 37°C.

To evaluate pleiotropic stress responses, strains were grown on YPD supplemented with caffeine at concentrations of 0.04mM, 0.075mM, and 0.1mM. Cell membrane stress was assessed using YPD supplemented with SDS at 0.04%, 0.075%, and 0.1%. Oxidative stress conditions were evaluated using YPD supplemented with H_2O_2 at 5mM, 10mM, and 15mM. Antifungal susceptibility assays included YPD supplemented with caspofungin (CSP) at 0, 1.5, 2.0, and 3.0µg/mL as an echinocandin-class fungicidal drug, and YPD supplemented with fluconazole (FLC)

at 0, 8, 16, 32, and 64µg/mL as an azole-class fungistatic drug. All plates were incubated at 30°C for 48 hours and subsequently photographed using the Bio-Rad Gel Doc XR+® documentation system.

6. Evaluation of contemporaneous strains from P10 on non-fermentable carbon sources

To further evaluate the possible mitochondrial dysfunction suggested by the phenotypic characterization assays, the contemporaneous isolates from P10 were subjected to additional drop-spot assays using non-fermentable carbon sources. Each contemporaneous isolate was inoculated into YPD broth and incubated for 48 hours at 30°C with constant shaking. After incubation, cultures were adjusted to an OD600 of 0.05 using sterile water and subjected to spot-growth assays under glycerol (YPG) and ethanol (YPE). We also performed a colorimetric assay using triphenyltetrazolium chloride (TTC). This assay produces either white or pink-red colonies, where white colonies indicate the inability to reduce TTC and therefore suggest defective mitochondrial respiratory activity [39]. All plates were incubated at 30°C for 48 hours and subsequently photographed.

7. MIC_{50} assays for P6 contemporaneous strains

To evaluate the growth differences observed among the P6 contemporaneous isolates in response to antifungal agents, we first analyzed their growth kinetics in liquid YPD medium under non-stress conditions for 25 hours using the area under the curve (AUC) method. Using the same approach, the minimum inhibitory concentration 50 (MIC_{50}) for FLC was determined for each contemporaneous isolate from P6.

The range of FLC concentrations tested was adapted according to the methodology reported by the Clinical and Laboratory Standards Institute (CLSI) (FLC: 0, 0.0312, 0.125, 0.5, 1, 2, 4, 8, 16, 20, 32, and 64µg/mL), prepared as 2X stock solutions in YPD medium. The contemporaneous clinical strains from P6 (AN264, AN359, AN812–AN821) were inoculated in YPD medium and incubated at 30°C. After 24 hours, 10µL of saturated culture was transferred into 5ml of fresh YPD medium and incubated again at 30°C for 48 hours. For experimental setup, cells were adjusted to an OD_{600} of 0.005 in YPD medium. Interactions with FLC were carried out in specialized plates for the Microbiology Reader Bioscreen C© system by combining

100µl of cell suspension with 100µl of the corresponding FLC stock solution, resulting in a final cellular OD_{600} of 0.0025 per well and a final antifungal concentration of 1X. Optical density measurements were recorded every 20 minutes for 25 hours at 30°C under constant agitation. Data analysis was performed using GraphPad Prism®.

After characterizing the general growth behavior of the contemporaneous groups, two representative contemporaneous isolates derived from each parental isolate were selected to further evaluate their interaction with three of the most used antifungal agents in clinical practice. MIC_{50} assays were performed following the protocol established by the European Society of Clinical Microbiology and Infectious Diseases (EUCAST, Definitive Document E.Def 7.4) for FLC, caspofungin (CSP), and micafungin (MICA) in Roswell Park Memorial Institute (RPMI) because it is a fully defined synthetic medium, commercially available with minimal batch-to-batch variation, which reduces an important source of variability in susceptibility testing [42].

The antifungal concentrations tested were as follows:

- FLC: 0, 0.5, 1, 2, 4, 8, 16, 20, 32, and 64µg/ml.
- CSP: 0, 0.0062, 0.0125, 0.025, 0.05, 0.1, 0.5, 1, 2, and 4µg/ml.
- MICA: 0, 0.0062, 0.0125, 0.025, 0.05, 0.1, 0.25, 0.5, 0.75, and 1µg/ml.

Antifungal solutions were prepared as 2X stocks in RPMI supplemented with 2% glucose for subsequent experimental setup. The contemporaneous clinical strains from P6 (AN264, AN359, AN812–AN821) were inoculated into RPMI medium and incubated at 30°C. After 24 hours, 10µl of saturated culture was transferred into 5ml of fresh RPMI medium and incubated at 30°C for 48 hours. Subsequently, 1ml of cells from each inoculum was collected, washed three times with Milli-Q water, and resuspended in 1ml of RPMI medium. Cell suspensions were then adjusted to an OD_{600} of 0.15 in 5ml of RPMI. From this suspension, 1ml was transferred into a new tube containing 4ml of RPMI. A total of 100µl of the adjusted cell suspension was dispensed into each well of a round-bottom plate, corresponding to approximately 60K cells per well. Additionally, 100µl of the corresponding antifungal stock solution was added to each well. Plates were incubated statically at 30°C. After 24 hours, cells were resuspended, and OD_{600} measurements were recorded using an

EPOCHH Plate Spectrophotometer, BioTek Instruments, Inc©. Data were analyzed using spreadsheet software and represented using GraphPad Prism®.
MIC_{50} values were determined for the selected contemporaneous isolates as well as for the laboratory reference strains for each of the three antifungal agents.

Statement on the use of IA

During the development of this work, artificial intelligence tools were used as academic and technical support. Scopus AI and Perplexity were used to search, filter, and summarize scientific information related to the topic. Specifically, Consensus helped obtain evidence-based summaries from previous research, while Perplexity was used to answer specific questions and identify complementary sources. On the other hand, ChatGPT was used exclusively to review the writing and improve the style of the text in order to enhance clarity and coherence, without modifying the interpretation of the results or the conclusions of the work.

References

1. Arastehfar A, Lass-Flörl C, Garcia-Rubio R, Daneshnia F, Ilkit M, Boekhout T, et al. The Quiet and Underappreciated Rise of Drug-Resistant Invasive Fungal Pathogens. J Fungi. 2020;6: 138. doi:10.3390/jof6030138

2. Fisher MC, Henk DanielA, Briggs CJ, Brownstein JS, Madoff LC, McCraw SL, et al. Emerging fungal threats to animal, plant and ecosystem health. Nature. 2012;484: 186–194. doi:10.1038/nature10947

3. Bitar D, Lortholary O, Le Strat Y, Nicolau J, Coignard B, Tattevin P, et al. Population-Based Analysis of Invasive Fungal Infections, France, 2001–2010. Emerg Infect Dis. 2014;20: 1163–1169. doi:10.3201/eid2007.140087

4. Brown GD, Denning DW, Gow NAR, Levitz SM, Netea MG, White TC. Hidden Killers: Human Fungal Infections. Sci Transl Med. 2012;4. doi:10.1126/scitranslmed.3004404

5. Carreté L, Ksiezopolska E, Gómez-Molero E, Angoulvant A, Bader O, Fairhead C, et al. Genome Comparisons of Candida glabrata Serial Clinical Isolates Reveal Patterns of Genetic Variation in Infecting Clonal Populations. Front Microbiol. 2019;10: 112. doi:10.3389/fmicb.2019.00112

6. Kullberg BJ, Arendrup MC. Invasive Candidiasis. Campion EW, editor. N Engl J Med. 2015;373: 1445–1456. doi:10.1056/NEJMra1315399

7. Pfaller MA, Diekema DJ, Turnidge JD, Castanheira M, Jones RN. Twenty Years of the SENTRY Antifungal Surveillance Program: Results for Candida Species From 1997–2016. Open Forum Infect Dis. 2019;6: S79–S94. doi:10.1093/ofid/ofy358

8. WHO Fungal Priority Pathogens List to Guide Research, Development and Public Health Action. 1st ed. Geneva: World Health Organization; 2022.

9. Hirakawa MP, Martinez DA, Sakthikumar S, Anderson MZ, Berlin A, Gujja S, et al. Genetic and phenotypic intra-species variation in *Candida albicans*. Genome Res. 2015;25: 413–425. doi:10.1101/gr.174623.114

10. Lim HJ, Choi MJ, Byun SA, Won EJ, Park JH, Choi YJ, et al. Whole-Genome Sequence Analysis of Candida glabrata Isolates from a Patient with Persistent Fungemia and Determination of the Molecular Mechanisms of Multidrug Resistance. J Fungi. 2023;9: 515. doi:10.3390/jof9050515

11. Frías-De-León MG, Hernández-Castro R, Conde-Cuevas E, García-Coronel IH, Vázquez-Aceituno VA, Soriano-Ursúa MA, et al. Candida glabrata Antifungal Resistance and Virulence Factors, a Perfect Pathogenic Combination. Pharmaceutics. 2021;13: 1529. doi:10.3390/pharmaceutics13101529

12. Seider K, Gerwien F, Kasper L, Allert S, Brunke S, Jablonowski N, et al. Immune Evasion, Stress Resistance, and Efficient Nutrient Acquisition Are Crucial for Intracellular Survival of Candida glabrata within Macrophages. Eukaryot Cell. 2014;13: 170–183. doi:10.1128/EC.00262-13

13. Takashima M, Sugita T. Taxonomy of Pathogenic Yeasts Candida, Cryptococcus, Malassezia, and Trichosporon: Current Status, Future Perspectives, and Proposal for Transfer of Six Candida Species to the Genus Nakaseomyces.

14. Gabaldón T, Carreté L. The birth of a deadly yeast: tracing the evolutionary emergence of virulence traits in *Candida glabrata*. Fairhead C, editor. FEMS Yeast Res. 2016;16: fov110. doi:10.1093/femsyr/fov110

15. López-Fuentes E, Gutiérrez-Escobedo G, Timmermans B, Van Dijck P, De Las Peñas A, Castaño I. Candida glabrata's Genome Plasticity Confers a Unique Pattern of Expressed Cell Wall Proteins. J Fungi. 2018;4: 67. doi:10.3390/jof4020067

16. Castanheira M, Messer SA, Rhomberg PR, Pfaller MA. Antifungal susceptibility patterns of a global collection of fungal isolates: results of the SENTRY Antifungal Surveillance Program (2013). Diagn Microbiol Infect Dis. 2016;85: 200–204. doi:10.1016/j.diagmicrobio.2016.02.009

17. Rubin LG. Bacterial Colonization and Infection Resulting from Multiplication of a Single Organism. Clin Infect Dis. 1987;9: 488–493. doi:10.1093/clinids/9.3.488

18. Cheng S, Fleres G, Chen L, Liu G, Hao B, Newbrough A, et al. Within-Host Genotypic and Phenotypic Diversity of Contemporaneous Carbapenem-Resistant Klebsiella pneumoniae from Blood Cultures of Patients with Bacteremia. Wright GD, editor. mBio. 2022;13: e02906-22. doi:10.1128/mbio.02906-22

19. Cornforth DM, Matthews A, Brown SP, Raymond B. Bacterial Cooperation Causes Systematic Errors in Pathogen Risk Assessment due to the Failure of the Independent Action Hypothesis. Schneider DS, editor. PLOS Pathog. 2015;11: e1004775. doi:10.1371/journal.ppat.1004775

20. Robbins N, Caplan T, Cowen LE. Molecular Evolution of Antifungal Drug Resistance. Annu Rev Microbiol. 2017;71: 753–775. doi:10.1146/annurev-micro-030117-020345

21. López-Marmolejo AL, Hernández-Chávez MJ, Gutiérrez-Escobedo G, Selene Herrera-Basurto M, Mora-Montes HM, De Las Peñas A, et al. Microevolution of Candida glabrata (Nakaseomyces glabrata) during an infection. Fungal Genet Biol. 2024;172: 103891. doi:10.1016/j.fgb.2024.103891

22. Ene IV, Farrer RA, Hirakawa MP, Agwamba K, Cuomo CA, Bennett RJ. Global analysis of mutations driving microevolution of a heterozygous diploid fungal pathogen. Proc Natl Acad Sci. 2018;115. doi:10.1073/pnas.1806002115

23. Badrane H, Cheng S, Dupont CL, Hao B, Driscoll E, Morder K, et al. Genotypic diversity and unrecognized antifungal resistance among populations of Candida glabrata from positive blood cultures. Nat Commun. 2023;14: 5918. doi:10.1038/s41467-023-41509-x

24. Foulet F, Nicolas N, Eloy O, Botterel F, Gantier J-C, Costa J-M, et al. Microsatellite Marker Analysis as a Typing System for *Candida glabrata*. J Clin Microbiol. 2005;43: 4574–4579. doi:10.1128/JCM.43.9.4574-4579.2005

25. Karaoglu H, Lee CMY, Meyer W. Survey of Simple Sequence Repeats in Completed Fungal Genomes. Mol Biol Evol. 2005;22: 639–649. doi:10.1093/molbev/msi057

26. Raposo CJ, McElroy KA, Fuchs SM. The Epithelial adhesin 1 tandem repeat region mediates protein display through multiple mechanisms. FEMS Yeast Res. 2020;20: foaa018. doi:10.1093/femsyr/foaa018

27. Alves R, Barata-Antunes C, Casal M, Brown AJP, Van Dijck P, Paiva S. Adapting to survive: How Candida overcomes host-imposed constraints during human colonization. Filler SG, editor. PLOS Pathog. 2020;16: e1008478. doi:10.1371/journal.ppat.1008478

28. Dellière S, Healey K, Gits-Muselli M, Carrara B, Barbaro A, Guigue N, et al. Fluconazole and Echinocandin Resistance of Candida glabrata Correlates Better with Antifungal Drug Exposure Rather than with MSH2 Mutator Genotype in a French Cohort of Patients Harboring Low Rates of Resistance. Front Microbiol. 2016;7. doi:10.3389/fmicb.2016.02038

29. Arendrup MC, Friberg N, Mares M, Kahlmeter G, Meletiadis J, Guinea J, et al. How to interpret MICs of antifungal compounds according to the revised clinical breakpoints v. 10.0 European committee on antimicrobial susceptibility testing (EUCAST). Clin Microbiol Infect. 2020;26: 1464–1472. doi:10.1016/j.cmi.2020.06.007

30. Pfaller MA, Castanheira M, Messer SA, Rhomberg PR, Jones RN. Comparison of EUCAST and CLSI broth microdilution methods for the susceptibility testing of 10 Systemically active antifungal agents when tested against Candida spp. Diagn Microbiol Infect Dis. 2014;79: 198–204. doi:10.1016/j.diagmicrobio.2014.03.004

31. Chesdachai S, Yetmar ZA, Ranganath N, Everson JJ, Wengenack NL, Abu Saleh OM. Antifungal Susceptibility Pattern of Candida glabrata from a Referral Center and Reference Laboratory: 2012–2022. J Fungi. 2023;9: 821. doi:10.3390/jof9080821

32. Pfaller MA, Andes D, Diekema DJ, Espinel-Ingroff A, Sheehan D. Wild-type MIC distributions, epidemiological cutoff values and species-specific clinical breakpoints for fluconazole and Candida: Time for harmonization of CLSI and EUCAST broth microdilution methods. Drug Resist Updat. 2010;13: 180–195. doi:10.1016/j.drup.2010.09.002

33. Jordà-Marcos R, Álvarez-Lerma F, Jurado M, Palomar M, Nolla-Salas J, León MA, et al. Risk factors for candidaemia in critically ill patients: a prospective surveillance study*. Mycoses. 2007;50: 302–310. doi:10.1111/j.1439-0507.2007.01366.x

34. Gülmez D, Alp S, Gursoy G, Ayaz CM, Dogan O, Arikan-Akdagli S, et al. Mixed fungaemia: an 18-year report from a tertiary-care university hospital and a systematic review. Clin Microbiol Infect. 2020;26: 833–841. doi:10.1016/j.cmi.2020.03.030

35. Vandeputte P, Tronchin G, Rocher F, Renier G, Bergès T, Chabasse D, et al. Hypersusceptibility to Azole Antifungals in a Clinical Isolate of *Candida glabrata* with Reduced Aerobic Growth. Antimicrob Agents Chemother. 2009;53: 3034–3041. doi:10.1128/AAC.01384-08

36. Peng Y, Dong D, Jiang C, Yu B, Wang X, Ji Y. Relationship between respiration deficiency and azole resistance in clinical Candida glabrata. FEMS Yeast Res. 2012;12: 719–727. doi:10.1111/j.1567-1364.2012.00821.x

37. Tanaka J, Kiyoshi K, Kadokura T, Suzuki K, Nakayama S. Elucidation of the enzyme involved in 2,3,5-triphenyl tetrazolium chloride (TTC) staining activity and the relationship between TTC staining activity and fermentation profiles in Saccharomyces cerevisiae. J Biosci Bioeng. 2021;131: 396–404. doi:10.1016/j.jbiosc.2020.12.001

38. Duvenage L, Munro C, Gourlay C. High Resolution Respirometry in Candida albicans. BIO-Protoc. 2019;9. doi:10.21769/BioProtoc.3361

39. Rich PR, Mischis LA, Purton S, Wiskich JT. The sites of interaction of triphenyltetrazolium chloride with mitochondrial respiratory chains. FEMS Microbiol Lett. 2001;202: 181–187. doi:10.1111/j.1574-6968.2001.tb10801.x

40. Huang S-J, Lv G, Song Y-H, Zhao J-T, Liu J-Y, Wang L-L, et al. Antifungal susceptibility, molecular epidemiology, and clinical risk factors of Candida glabrata in intensive care unit in a Chinese Tertiary Hospital. Front Cell Infect Microbiol. 2024;14: 1455145. doi:10.3389/fcimb.2024.1455145

41. Alexander BD, Johnson MD, Pfeiffer CD, Jiménez-Ortigosa C, Catania J, Booker R, et al. Increasing Echinocandin Resistance in Candida glabrata: Clinical Failure Correlates With Presence of FKS Mutations and Elevated Minimum Inhibitory Concentrations. Clin Infect Dis. 2013;56: 1724–1732. doi:10.1093/cid/cit136

42. Sasoni N, Caracciolo B, Cabeza MS, Gamarra S, Carnovale S, Garcia-Effron G. Antifungal susceptibility testing following the CLSI M27 document, along with the measurement of MFC/MIC ratio, could be the optimal approach to detect amphotericin B resistance in *Clavispora* (*Candida*) *lusitaniae* . Susceptibility patterns of contemporary isolates of this species. Groll AH, editor. Antimicrob Agents Chemother. 2024;68: e00968-23. doi:10.1128/aac.00968-23

43. Cormack BP, Ghori N, Falkow S. An Adhesin of the Yeast Pathogen *Candida glabrata* Mediating Adherence to Human Epithelial Cells. Science. 1999;285: 578–582. doi:10.1126/science.285.5427.578

44. Fidel PL, Cutright JL, Tait L, Sobel JD. A Murine Model of Candida glabrata Vaginitis. J Infect Dis. 1996;173: 425–431. doi:10.1093/infdis/173.2.425

Supporting information

S1 Table. List of *C. glabrata* control strains used in this study.

Strain	Parental strain	Genotype	Phenotype	Description
BG14 (CGM1)	BG2	*ura3*Δ::Tn903	Ura- Gly+ FLC^{SDD}	BG2 *ura3*Δ::Tn903 [43]
CBS (CBS138)	WT	ATCC2001	Ura+ Gly+	Clinical isolate, [44].
AN376	WT	*fen1* (Y220C)	Ura+ CSP^{R}	Clinical isolate from urine from P7
AN378	WT	*PDR1* (G1099C)	Ura+ FLC^{R}	Clinical isolate from blood from P7
CGM1938	BG14	*ura3*Δ::Tn903	Ura- Gly-	Petite obtained by EtBr from BG14
CGM1939	BG14	*ura3*Δ::Tn903	Ura- Gly-	Petite obtained by EtBr from BG14

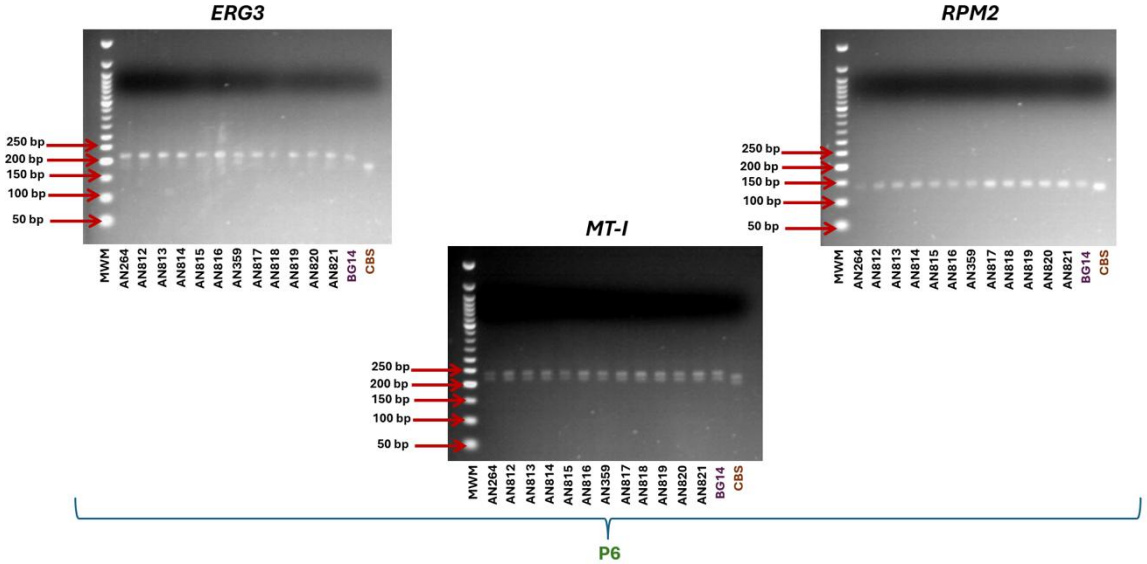

S1 Fig. Genotyping with *ERG3, RPM2,* and *MT-I* molecular markers from P6. No variation in PCR product size was detected among the contemporaneous strains for any of the evaluated markers; however, their amplification profiles differed from those observed in the CBS138 and BG14 reference strains.

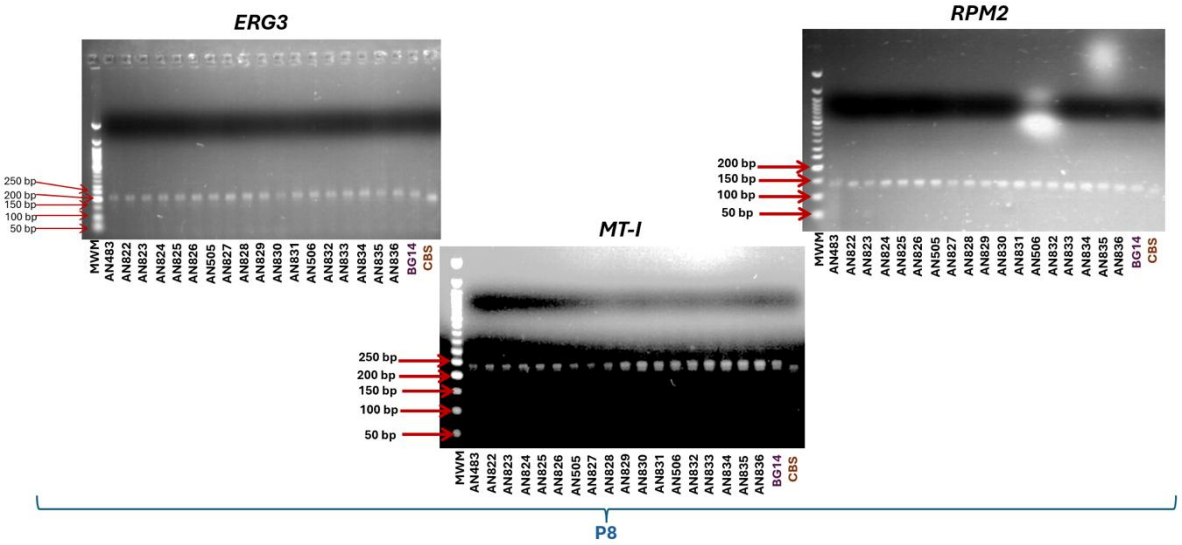

S2 Fig.. Genotyping with *ERG3, RPM2,* and *MT-I* molecular markers from P8. No variation in PCR product size was detected among the contemporaneous strains for any of the evaluated markers; however, their amplification profiles differed from those observed in the CBS138 and BG14 reference strains.

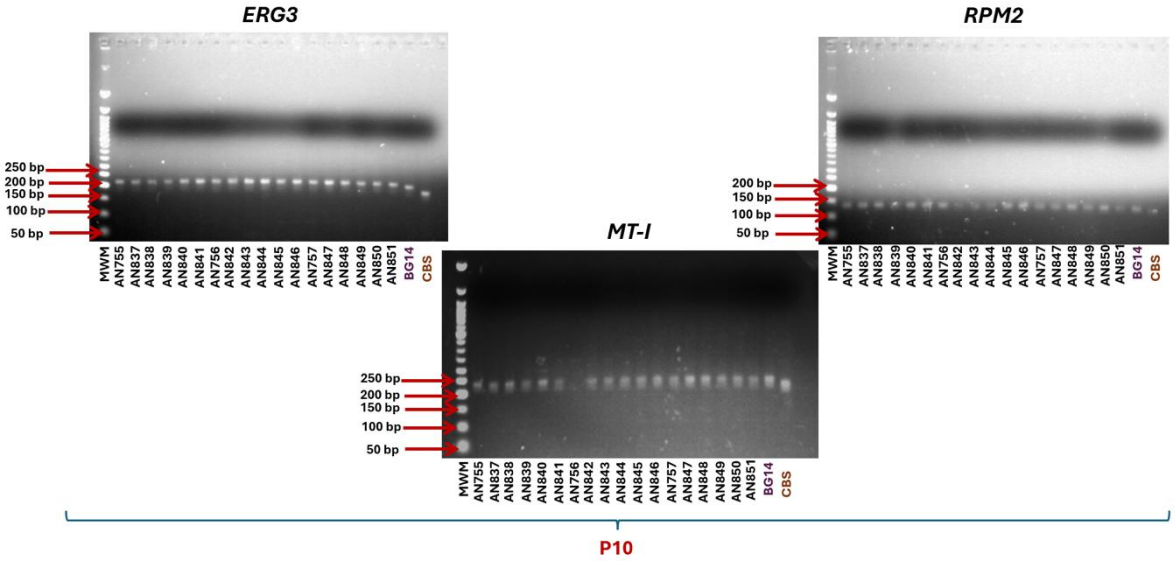

S3 Fig. Genotyping with *ERG3, RPM2,* and *MT-I* molecular markers from P10.

No variation in PCR product size was detected among the contemporaneous strains for any of the evaluated markers; however, their amplification profiles differed from those observed in the CBS138 and BG14 reference strains.

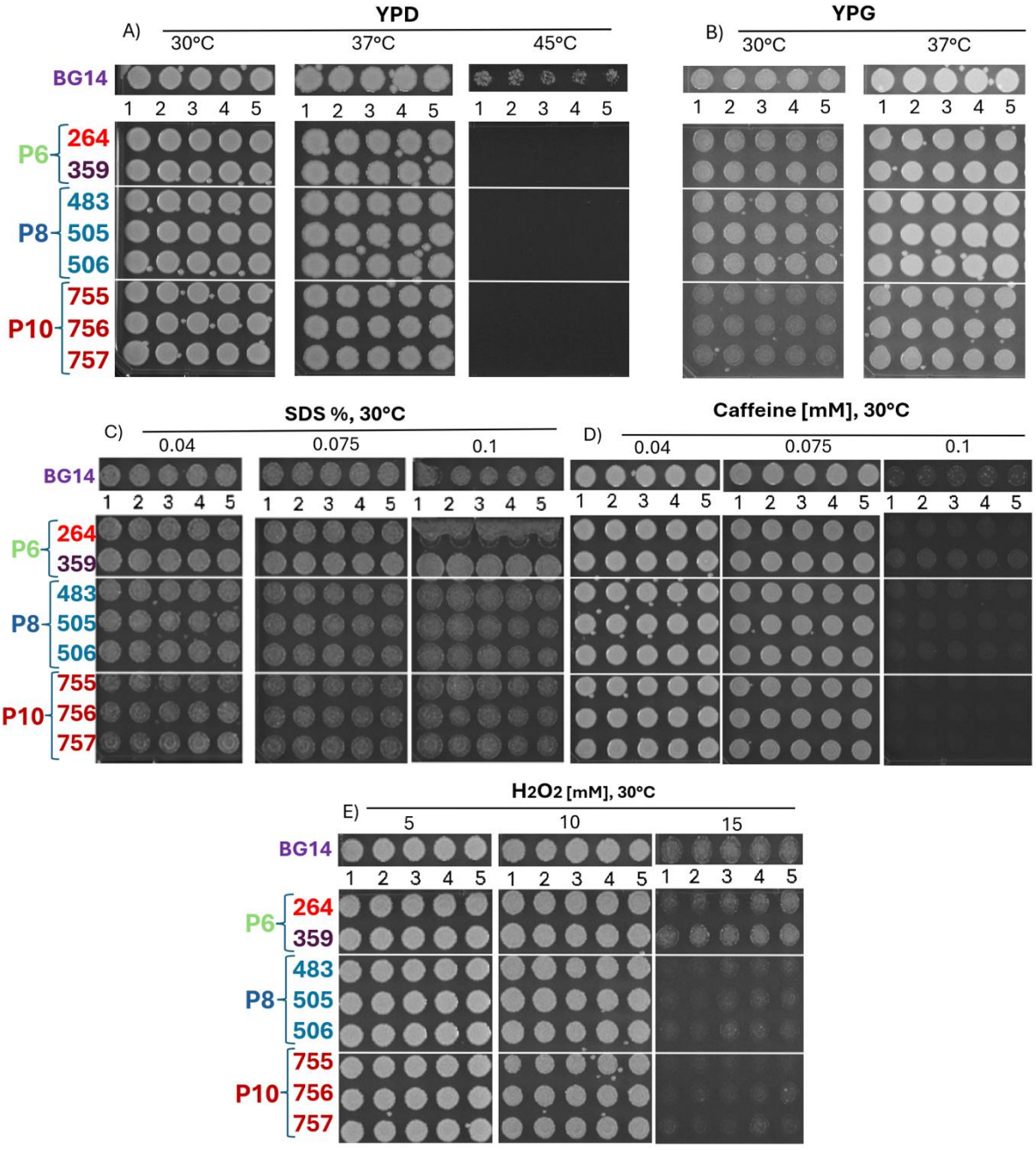
A)
YPD
30°C
37°C
45°C
B)
YPG
30°C
37°C
BG14
1 2 3 4 5
P6
264
359
P8
483
505
506
P10
755
756
757
C)
SDS %, 30°C
0.04
0.075
0.1
D)
Caffeine [mM], 30°C
0.04
0.075
0.1
E)
H2O2 [mM], 30°C
5
10
15

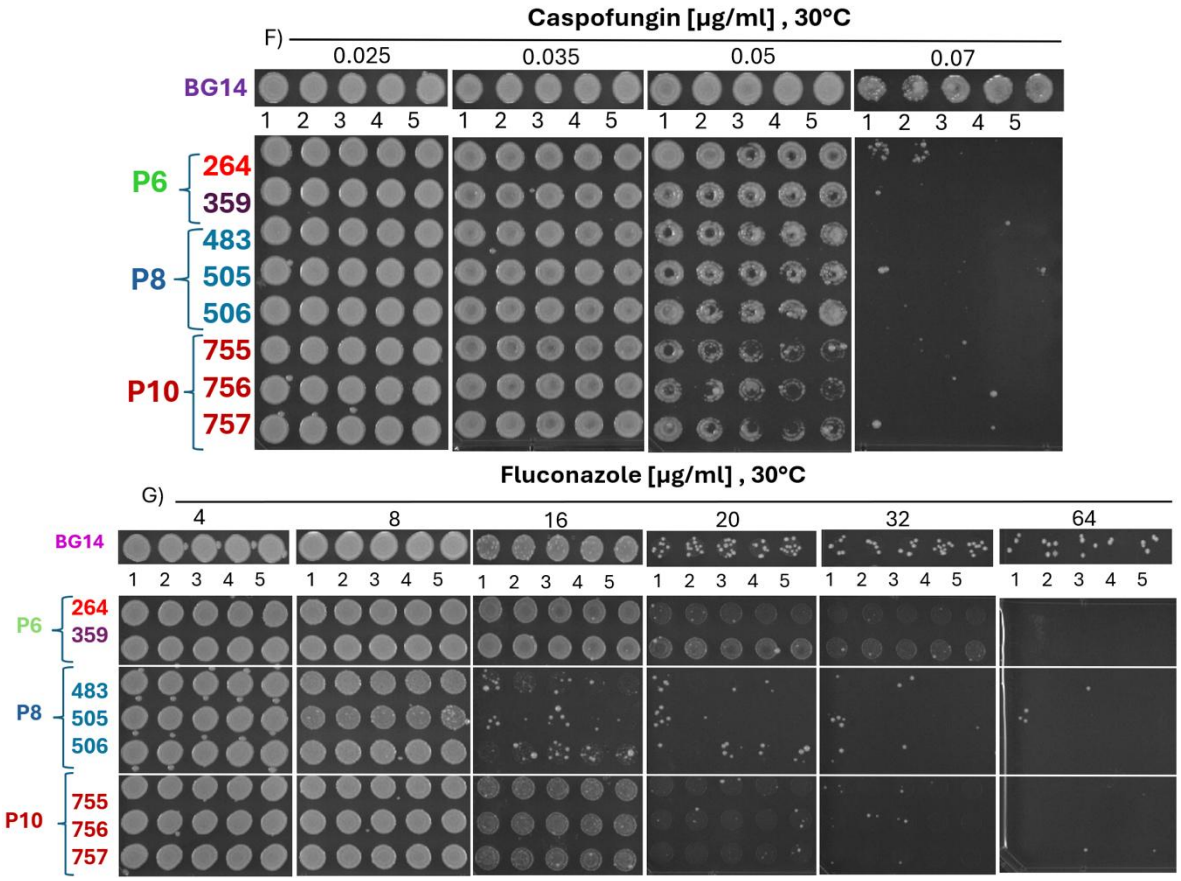

S1 Fig.. Succeptibility assays under differents types of stressors in contemporaneous clinical strains in P6, P8 and P10.

Phenotypic characterization was performed for the 40 contemporaneous isolates obtained from the three patients (P6, P8 and P10). Each new *C. glabrata* isolate was inoculated into YPD broth and incubated for 48 hours at 30°C with shaking. After incubation, cultures were adjusted to an OD_{600} of 0.05 using sterile water and subjected to spot-growth assays under different stress and drug susceptibility conditions. Growth on YPD plates at 30°C was used as the control condition, while growth at 37°C and 45°C was evaluated as thermal stress (A). We also assessed growth on YPG medium containing 3% glycerol instead of dextrose as a non-fermentable carbon source at both 30°C and 37°C (B). Cell membrane stress was assessed using YPD supplemented with SDS at 0.04%, 0.075%, and 0.1% (C). To evaluate pleiotropic stress responses, strains were grown on YPD supplemented with caffeine at concentrations of 0.04mM, 0.075mM, and 0.1Mm (D). Oxidative stress conditions were evaluated using YPD supplemented with H_2O_2 at 5mM, 10mM, and 15mM (E). Antifungal susceptibility assays included YPD supplemented with caspofungin (CSP) at 0, 1.5, 2.0, and 3.0µg/mL as an echinocandin-class fungicidal drug (F), and YPD supplemented with fluconazole (FLC) at 0, 8, 16, 32, and 64µg/mL as an azole-class fungistatic drug(G). All plates were incubated at 30°C for 48 hours and subsequently photographed using the Bio-Rad Gel Doc XR+ documentation system. Representative photographs of three biological and independent assays.